Received: 18 January 2024 | Revised: 29 April 2024 | Accepted: 22 May 2024

IET Energy Systems Integration

DOI: 10.1049/esi2.12152

ORIGINAL RESEARCH

An integrated planning framework for optimal power generation portfolio including frequency and reserve requirements

Olayinka Ayo[1] | Paola Falugi[1,2] | Goran Strbac[1]

[1]Department of Electrical and Electronic Engineering, Imperial College London, London, UK

[2]Department of Engineering & Construction, University of East London, London, UK

Correspondence

Olayinka Ayo.
Email: omowunmiayo@gmail.com

Abstract

Electricity system decarbonisation poses several challenges to network stability and supply security, given renewables' intermittency and possible reduction of system inertia. This manuscript presents a novel integrated system framework to determine optimal generation investments for addressing decarbonisation challenges and achieving cost-effective electricity systems while ensuring frequency stability and reserve requirements are met at the operational level in a net-zero system. The novel planning framework is a mixed-integer bilinear programming problem accurately modelling clustered variables for the on/off status of generation units and seconds-timescale frequency requirements at an operational and planning level. The benefits of the decision framework and effects of dispatch decisions in a year are illustrated using the Great Britain case study. The results provide optimal trade-offs and cost-effective investment portfolios for including detailed modelling of unit-commitment and frequency stability constraints versus not including them in the planning model. Making investment decisions for a net-zero electricity system without these constraints can lead to very high system costs due to significant demand curtailment. Although the model's computation burden was increased by these constraints, complexity was managed by formulating them tightly and compactly. Non-convex quadratic nadir constraints were efficiently solvable to global optimality by applying McCormick relaxations and branching techniques in an advanced solver.

KEYWORDS

frequency control, optimisation, power generation planning, power generation scheduling, power system economics

1 | INTRODUCTION

The ambitious decarbonisation targets agreed upon by countries globally are bringing about significant transitions in technology investments and operations of power system networks. Achieving a low or net-zero emission system requires substantial additions of variable, non-synchronous, low-carbon generators and the retirement of many conventional power plants [1–3]. In a bid to achieve supply security with variable and unpredictable renewable energy generators, enormous complexities are being imposed on the system. From the system operator perspective, the low-inertia nature of a network with high penetration of intermittent renewable energy generators would require more reserves and flexibility to provide an adequate frequency response and ancillary services [1, 2, 4, 5]. Providing these services with conventional generators increases the chances of renewable power curtailment, especially during high output at off-peak times and in violation of emission targets, thereby increasing costs in the system. These challenges, therefore, highlight a need for cost-effective

Abbreviations: Bn, Billion; CCGT, Combined cycle gas turbine; CCS, Carbon Capture and Storage; CUC, Clustered Unit Commitment; EFR, Enhanced Frequency Response; GB, Great Britain; GHR, Gas heated reformer; H, Hours; H_2, Hydrogen; H_2CCGT, Hydrogen combined cycle gas turbine; IC, Investment costs; LHS, Left-hand side; M, Minutes; MILP, Mixed Integer Linear Programming; MIP, Mixed Integer Programming; NP, Non-deterministic Polynomial time; OC, Operational costs; PFR, Primary Frequency Response; RHS, Right-hand side; RoCoF, Rate of change of frequency; UC, Unit commitment; Yr, Year.

investment decisions in flexible technology solutions to attain supply security in future integrated low-carbon power systems. The whole system assessment of power systems networks has been shown to improve the cost-effectiveness of investments and operations of technologies [6, 7].

Even though some authors [8] highlight that modelling unit commitment (UC) may not be relevant in a system with almost 100% renewables penetration, there are increasingly more flexible, clean firm technologies, such as hydrogen technologies, nuclear, biogas, and natural gas with carbon capture and storage (CCS) technology, necessary for reliability and balancing services in the future net-zero carbon electricity system [9]. Literature has shown that in a system with high penetration of variable renewable sources, modelling UC constraints and online status of generators at the operational level are key for capturing the needed system flexibility, amongst other critical requirements such as reserves and temporal constraints [10]. Some recent research works have shown the importance of operational details in an investment planning model [11]. However, only a few existing research studies have considered an integrated expansion planning problem of power systems, including detailed operational constraints, especially inter-temporal constraints such as UC, frequency, and reserve constraints. The few existing studies formulate the integrated expansion problem by adopting a considerably simplified description of the operational level. In a bid to highlight the benefits of UC constraints modelling, the authors in Ref. [11] showed hourly ramping rate constraints make for more cost-effective generation expansion decisions but excluded other relevant generator characteristics such as the start-up/down cost or minimum-up & down time. However, such investment models do not adequately describe the value and potential of flexibility in power system technologies. The authors in Refs. [12, 13] emphasise the benefits of power-based unit-commitment modelling to accurately represent flexibility capabilities and system requirements, as they ensure more effective use of the installed generator investments when compared with an energy-based model. Specifically, the authors in Ref. [14] highlighted that the tight and compact formulation of UC, amongst the current state-of-the-art formulations, is more computationally efficient for solving day-ahead dispatch of generation units.

More so, the authors in Refs. [13, 15] proved that not including UC constraints leads to overestimating the value and actual flexibility required from synchronous, renewable, and flexible technologies and underestimating the operational and total system cost. Neglecting UC constraints significantly affects the capacity mix deemed optimal by the model, the resulting generation mix, carbon emissions and cost projections, specifically for a highly renewable and carbon-constrained electricity system. This study focuses on capturing the operational flexibility of these more flexible power plants and flexible technologies in a planning model for accurate and cost-effective investments. Also, to replicate the ramping, reserve, start-up/shut-down flexibility of individual UC within a cluster, the authors in Ref. [16] has proposed a more accurate method for formulating clustered power-based UC, which will be adopted in this paper. The formulation includes constraints with the binary on/off status and reserve assignment for individual units of clustered generators with identical technology to avoid overestimating their flexibility in a system with the high penetration of variable renewable sources without increasing the computational burden.

Systems operators require flexibility to provide ancillary services, especially reserves and frequency response, balancing supply-demand deviations and essential system requirements in future power systems planning models. Increasingly, system operators need to procure more frequency response products such as systems inertia, Enhanced Frequency Response (EFR), and primary frequency response to handle the growing low inertia in the projected renewable energy-dominated system. A report by the National Grid [17] proposed the need for sub-second, faster-acting response services from alternative technologies to conventional thermal plants to achieve optimum flexibility in power systems with decreasing inertia. The frequency response requirements on a system depend on the available system inertia and the size of the largest generator loss. Battery storage systems have been shown to provide the much-required sub-second response [17, 18]. Through a novel frequency-constrained stochastic UC model, the authors in Ref. [19] further showed the benefits of co-optimising energy production and provision of synchronised and synthetic inertia, EFR, Primary Frequency Response (PFR) and dynamically-reduced largest power in-feed. In addition, the authors in Ref. [20] proved the capability of a Combined Cycle Gas Turbine Plant (CCGT) to provide the much-needed flexibility for future low-carbon power systems, especially those with enhanced flexibility parameters. Some studies have recognised the importance of including these frequency stability requirements in investment planning problems. The authors Ref. [21] in their article on assessing the impact of inertia and reactive power constraints in generation expansion planning emphasised that disregarding inertia and reactive power constraints in generation expansion planning formulations can result in extra costs, load curtailment, and distortion of optimal resource allocation. However, their article did not consider the frequency stability constraints.

The authors in Refs. [6, 7] employed a whole system approach to determine the benefits of real-time balancing per second over a 1-year time horizon. The model emphasised savings that can come from co-optimising generation and network assets investment while improving the operational efficiency of different assets in the system. Frequency response and reserve provision from energy storage and conventional generators were considered without frequency-security constraints. In addition, the authors in Ref. [22] considered energy storage potential alongside conventional generators in the planning problem for primary frequency response adequacy and for improving the system's frequency security limits. This model did not consider the different response times of storage and conventional generators in providing frequency response. More specifically, these research studies excluded the detailed modelling of security constraints such as the primary frequency response (PFR) constraints, which can ensure the security of

supply at times of lower inertia and loss of the largest generator. The authors in Ref. [8] showed that in UC problems, the rate of change of frequency (RoCoF) limit is typically the most restrictive constraint in an inertia-aware binary UC problem, compared to the limits on frequency nadir and quasi-steady state frequency deviation. Studying the impacts of omitting and including these other FR constraints in a generation planning problem becomes essential.

The authors in Ref. [23] carried out studies on a planning problem, without detailed UC modelling, to identify the role of the fast frequency response of energy storage systems and renewable technologies for ensuring frequency stability in future low-inertia systems. The model included inertia and RoCoF contributions and showed some benefits, but inertia was fixed for different studies without considering the number of generators online. Similarly, the authors in Ref. [10] examined the impact of operational details on generation investment planning in a renewable energy-dominated system. The model included ramping limits, UC and very fast frequency containment reserves requirements in inertia and RoCoF. However, apart from the integer UC variable being relaxed to its linear counterpart, the research did not consider ramping costs, shutdown costs, or different start-up types. Also, the frequency stability constraints adapted did not consider load damping effect, nadir, or quasi-steady state requirements, and the largest generator loss was a fixed value as a function of time.

Whilst these studies have investigated some level of operational details in their power system models, the current study includes additional details for assessing the impact of scheduling and frequency stability constraints on investments in technologies. The paper reports a comparative study of integrated planning problems that consider different formulations of scheduling constraints. Both planning problems employ a clustered UC formulation, but one of the formulations includes a detailed description of the commitment of the single generators.

2 | CONTRIBUTION AND APPROACH

This article proposes a novel integrated planning framework to determine the optimal technology portfolio for a cost-effective electricity system while ensuring frequency stability and reserve requirements at the operational level. The framework integrates the operational dynamics of post-fault frequency requirements [19] of the frequency rate of change, frequency nadir, and quasi-steady state frequency in an integrated planning problem formulation, selecting the optimal generation and flexible technologies portfolio. In order to meaningfully model the response limitations of conventional generators, we have adopted a detailed description of the inter-temporal constraints of each unit based on Ref. [24]. The accurate UC model allows considering simultaneous scheduling of multiple frequency services and identifying optimal investments in low-carbon technologies such as Hydrogen-powered CCGT (H_2CCGT), nuclear and renewable assets, as well as flexible technologies such as battery storage, hydrogen storage and electrolysers, which operate at multiple timescales, for the security of supply and stable operation of future power systems. However, using an accurate UC model in a planning problem, consisting of multiple investment options, services and timescales, gives rise to a challenging optimisation problem due to the substantial increase of symmetries. As a result, additional constraints removing a large proportion of the symmetries have been introduced to improve computational performances considerably. The resulting model is a large-scale mixed-integer bilinear programming problem solvable to global optimality by applying McCormick relaxations and spatial branching techniques implemented in the Gurobi optimisation solver [25].

To the best of the authors' knowledge, the proposed framework and relative case studies consider for the first time multiple post-fault seconds-timescale frequency requirements in an integrated planning problem formulation, including detailed descriptions of the inter-temporal constraints of each generator unit and contribution of different hydrogen and other flexible technologies for reserve and frequency provision services.

After applying the aforementioned linearisation techniques for bilinear constraints from using an advanced solver, the novel planning model becomes a mixed-integer linear programming problem optimised on a time horizon of 1 year and hourly time resolution consisting of discrete variables for Investment costs (IC) and binary variables for the on/off status of generation units at the operational level. The presented deterministic studies focus on a cost-benefit system analysis capturing the effects of dispatch decisions in 1 year from the central planner/utility point of view. The constraints formulated on the hourly variables include conditions happening on the time scales of seconds, especially for the frequency response requirements. Also, the requirements on an annual basis, such as the need for hydrogen to be stored across seasons for periods of low renewable output, are formulated with estimated boundary conditions but still using the hourly time horizon. The benefits of the proposed approach are depicted through modelling and analysing the technologies in a modified single-bus system to address some critical concerns about the role of storage and hydrogen technologies for the future power system. An extensive analysis of the impact of various system operational characteristics on generation expansion planning problems consisting of low-carbon conventional technologies, low-inertia renewable technologies, and flexible technologies has been performed to ensure system security and stability. The studies concurrently optimise investments in low-carbon technologies while minimising the system's short-term Operating costs (OC) through hourly time resolution representation of the system operation together with reserve and frequency stability and regulation requirements for a net-zero system. To the best of the authors' knowledge, the proposed study has not been conducted to the depth of modelling detail applied at the operation level of this planning problem.

A similar study was conducted by the authors in Ref. [10], where the impact of operational details on a single node generation investment planning in energy systems dominated by renewable plants was examined. However, apart from the integer UC variable being relaxed to its linear counterpart, the analysis did not also consider ramping costs, shut-down costs or different start-up types. Also, the frequency stability constraints adopted did not consider load damping effect, nadir or quasi-steady state requirements. The largest generator loss was also considered to be a fixed value per time.

In summary, the main contributions of this paper are as follows:

- We propose a model framework linking seconds-timescale frequency stability and hourly timescale UC to a yearly timescale generation planning optimisation.
- We examined the impact of detailed seconds-timescale frequency stability and mixed integer UC constraints, amongst other operational details, on the optimal planning for investments in technologies simultaneously scheduled to provide inertia, primary frequency response, and enhanced frequency reserves in a net-zero system.
- We also examined the integration of hydrogen technologies, especially H_2CCGT, for supporting the frequency response, amongst other flexibility requirements.
- We propose additional constraints to remove a large proportion of the symmetries introduced by the clustered UC variables to improve computational performances considerably.

All the studies consider the projected electricity and heating demand in the 2050 GBnet-zero scenario developed by the government [1] to emphasise the impacts and benefits of considering frequency stability constraints in a generation expansion planning problem.

3 | PROBLEM FORMULATION

The proposed system design problem follows an integrated system approach to power planning according to [7, 26] and captures the influence of fast dynamics at the investment temporal scale. The objective function to be minimised consists of the overall system costs (investment and operation cost) subject to investment and operation constraints:

$$\min_{x\in\mathcal{C}(\rho)} \left(V^I(x,\rho) + V^O(x,\rho)\right) \tag{1}$$

Equation (1) states both the investment cost function $V^I(\cdot)$ and operations cost function $V^O(\cdot)$ are to be minimised, where x denotes the whole collection of decision variables, ρ the system parameters and $\mathcal{C}(\cdot)$ the set of constraints depending on the parameters ρ. Refer to Appendix A for the nomenclature of the symbols used for the parameters and variables used in the problem formulation. The full set of constraints is introduced and discussed later in this section, while the investment cost function $V^I(\cdot)$ and operation cost function $V^O(\cdot)$ are as follows:

$$V^I(x,\rho) = \sum_{n\in\Omega_N}\left(\sum_{s\in\Omega_S}\kappa_s^H H_{n,s} + \sum_{r\in\Omega_R^T}\kappa_r^G R_{n,r} + \sum_{g_T\in\Omega_G^T}\kappa_{g_T}^H G_{n,g_T} + \sum_{el\in\Omega_{EL}^T}\kappa_{el}^H G_{n,el}^H + \sum_{bl\in\Omega_{BL}^T}\kappa_{bl}^H G_{n,bl}^H\right) \tag{2}$$

$$V^O(x,\rho) := \sum_{b\in\Omega_B} w_b \sum_{t\in\Omega_T^b}\left\{\Delta_t\left[\sum_{g\in\Omega_G}\left(c_g^G\left(p_{t,g}+p_g^{msg}u_{t,g}\right)+c_g^{nl}u_{t,g}\right) + \sum_{n\in\Omega_N}\left[\grave{\sigma}_{t,n}^d + \sum_{s\in\Omega_S}\left(c_s^+ h_{t,n,s}^+ + c_s^- h_{t,n,s}^-\right)\right]\right] + \sum_{n\in\Omega_N}\left(\sum_{el\in\Omega_{EL}^T} c_{el}Q_{t,n,el} + \sum_{bl\in\Omega_{BL}^T} c_{bl}Q_{t,n,bl}\right) + \sum_{g\in\Omega_G} c_g^{su}u_{t,g}^+ + c_g^{sd}u_{t,g}^- + \Upsilon R_t^{slack} + \sum_{g\in\Omega_G} c_{res}res_{t,g} + \sum_{g\in\Omega_G} c_{rsp}rsp_{t,g}\right\} \tag{3}$$

The investment cost function $V^I(\cdot)$ deals with the balance among renewable generation, thermal generators, storage assets, hydrogen production technologies such as gas-heated reformers with carbon capture storage (GHR-CCS) and electrolysers for blue and green hydrogen gas, respectively. The storage assets include both battery storage and hydrogen storage plants. The operation cost function $V^O(\cdot)$ consists of the sum of generation cost, start-up cost, no-load cost, shut-down cost, load curtailment, reserve curtailment, cost of reserve scheduling, [27], cost of hydrogen production, and storage operation costs. Load curtailment is economically penalised using the Value of Lost Load Γ, fixed at 30, 000 $\$/MWh$, while reserve curtailment is economically penalised using Υ.

Limitations on investment in thermal generation technologies are as follows:

$$0 \le G_{n,g_T} \le \overline{G}_{n,g_T}, \quad \forall g_T \in \Omega_G^T, \ \forall n \in \Omega_N \tag{4}$$

$$0 \le G_{n,o}^H \le \overline{G^H}_{n,o} \quad \forall\, o \in \Omega_{EL,BL}^T \ \forall\, n \in \Omega_N \tag{5}$$

Similar investment bounds have been imposed on other candidate technologies considered for investment in constraint (2).

Constraints (6) describe the supply demand balance $\forall\, n \in \Omega_N$, $\forall\, t \in \Omega_T^b$ and $\forall b \in \Omega_B$

$$\sum_{g\in\Omega_G} J_{n,g}\left(p_{t,g} + p_g^{msg} u_{t,g}\right) + \sum_{r\in\Omega_R} p_{t,n,r}^R + \sum_{\ell\in\Omega_\ell} I_{n,\ell} f_{t,\ell} + \sum_{es\in\Omega_S^E}\left(h_{t,n,es}^- - h_{t,n,es}^+\right) + \sigma_{t,n}^d = d_{t,n} + \frac{Q_{t,n,el}}{\eta_{el}} \tag{6}$$

In like manner, the supply demand operation of the electrolyser, GHR-CCS hydrogen technology, and hydrogen storage technologies per time is described in constraint (7) $\forall b \in \Omega_B$, $\forall\, t \in \Omega_T^b - \left\{t_b^+\right\}$ [28]:

$$\sum_{n\in\Omega_N}\left(Q_{t,n,el} + Q_{t,n,bl} + \sum_{hs\in\Omega_S^H}\left(h_{t,n,hs}^- - h_{t,n,hs}^+\right)\right) = \sum_{n\in\Omega_N}\left(J_{n,h2g}\frac{p_{t,h2g} + p_{h2g}^{msg} u_{t,h2g}}{\eta_{h2}}\right) \tag{7}$$

where $h2g$ indicates the H_2CCGT plants.

The LHS of supply demand constraints (7) includes the sum of hydrogen produced by the electrolyser, GHR-CCS, and hydrogen stored, while the RHS describes the demand for hydrogen driven by the electrical power output of the H_2CCGT plant. Note that in constraint (7), hydrogen transportation is neglected as the balance is performed by summing over all the bus nodes. The operation of the hydrogen production by the electrolyser and GHR-CCS is modelled as follows $\forall b \in \Omega_B$, $\forall\, t \in \Omega_T^b - \left\{t_b^+\right\}$ [28]:

$$0 \le Q_{t,n,el} \le G_{n,el}^H \quad \forall\, el \in \Omega_{EL}^T \;\; \forall\, n \in \Omega_N \tag{8}$$

$$0 \le Q_{t,n,bl} \le G_{n,bl}^H \quad \forall\, bl \in \Omega_{BL}^T \;\; \forall\, n \in \Omega_N \tag{9}$$

Constraints (8) and (9) describe the operational boundaries of the hydrogen produced by the electrolyser and GHR-CCS, respectively.

The limits and distribution of the power flow over the network are described by the following constraints $\forall b \in \Omega_B$, $\forall t \in \Omega_T^b$, and $\forall \ell \in \Omega_\ell$

$$f_{t,\ell} = \frac{1}{\chi_\ell}\left(\theta_{t,w_\ell} - \theta_{t,v_\ell}\right), \quad \left|f_{t,\ell}\right| \le F_\ell^0. \tag{10}$$

In this model, the line capacity for providing reserves is assumed to be available, and enough room is left in the lines for its provision. The provision of reserves is doubled based on the need to satisfy flow conditions and reserve provisions from different nodes.

3.1 | Storage operation

The storage operation is modelled as follows $\forall b \in \Omega_B$, $\forall\, t \in \Omega_T^b$ $\forall\, s \in \Omega_S$ and $\forall n \in \Omega_N$.

$$\tilde{h}_{t+1,n,s} = \tilde{h}_{t,n,s} + \Delta_t\left(\rho_s^+ h_{t,n,s}^+ - \frac{h_{t,n,s}^-}{\rho_s^-}\right) \tag{11}$$

$$\tilde{h}_{t_b^+,n,s} = \tilde{h}_{t_b^-+1,n,s} \tag{12}$$

$$0 \le h_{t,n,s}^- \le \hat{S}_{n,s}^- := \overline{S}_{n,s}\overline{h}_s + H_{0,s}^n \tag{13}$$

$$0 \le h_{t,n,s}^+ \le \hat{S}_{n,s}^+ := \overline{S}_{n,s}\overline{h}_s + H_{0,s}^n \tag{14}$$

$$0 \le \tilde{h}_{t,n,s} \le \hat{Z}_{n,s} := \overline{S}_{n,s}\overline{\eta}_s + \hat{Z}_{0,s}^n \tag{15}$$

where $H_{0,s}^n$, $H_{0,s}^n$ and $\hat{Z}_{0,s}^n$ describe the existing storage technology s at bus n. Constraint (11) computes the energy level of the storage for each time period. Constraint (12) assigns the energy level at the beginning of a block equal to the value at its end. The convex formulation of the storage constraints includes charge and discharge efficiency parameters $\left(\rho_s^+, \rho_s^-\right)$ which have values less than 100%. Since the efficiency value is less than one, there will be energy losses while cycling, limiting the occurrence of simultaneous charging and discharging [29]. In addition, a small cost of charging and discharging introduced in the objective function (2) has been introduced in the model as a penalty parameter [29]. Since the model considers losses and charging and discharging operation costs, the solutions with simultaneous charging and discharging are not optimal. Since hydrogen storage is seasonal, its behaviour follows an annual periodicity. It requires assigning the energy level at the beginning of the year equal to the energy level at the end of the year. Constraint (13)–(15) describes the limits on the charge, discharge, and energy level variables of the storage. To determine the initial storage condition for each temporal block and impose periodic annual conditions, we introduce a dynamic equation describing the energy accumulated or used during the year as follows:

$$\tilde{z}_{b+1,n,hs} = \tilde{z}_{b,n,hs} + w_b \sum_{t\in\Omega_T^b}\left(\Delta_t\left(\rho_{hs}^+ h_{t,n,hs}^+ - \frac{h_{t,n,hs}^-}{\rho_{hs}^-}\right)\right), \tag{16}$$

$$\tilde{z}_{1,n,hs} = \tilde{z}_{N_b+1,n,hs} \tag{17}$$

for temporal blocks $b = 1, \ldots, N_b + 1$. Constraints (16) estimate the energy level for each temporal block from the daily difference of total charge and discharge variables while constraint (17) is similar to constraint (12) but applied to the first temporal block in the year and the first time block in the

next year. The initial conditions for hydrogen storage are then defined by

$$\tilde{h}_{t_b^+,n,hs} = \tilde{z}_{b,n,hs}, \quad \forall b \in \Omega_b \tag{18}$$

Constraint (18) ensures that the energy level at the start of the day in a temporal block is equivalent to the total energy level at the beginning of its temporal block.

3.2 | Generator scheduling constraints

To represent the ability of different generation technology to provide frequency services, we need to take into account ramping limits, and for this reason, we model the on/off status of each thermal generation unit. Aggregate models of thermal generators do not accurately identify the ramping capability of the system because a feasible solution of the aggregate model does not imply the existence of a feasible solution for the current operating condition of every single generator. The integer UC formulation proposed in Refs. [16, 24, 30] has numerical advantages since the model is almost tight when the integrality constraints are relaxed. The thermal generators are required to satisfy minimum up/down times and logical constraints $\forall b \in \Omega_B$, $\forall t \in \Omega_T^b - \{t_b^+\}$, $\forall g \in \Omega_G$:

$$u_{t,g} - u_{t-1,g} = u_{t,g}^+ - u_{t,g}^-, \quad u_{t,g}, u_{t,g}^+, u_{t,g}^- \in \{0, 1, \ldots, N_g\} \tag{19}$$

$$\sum_{k=t-\hat{T}_g^U+1}^{t} u_{k,g}^+ \le u_{t,g} \quad \forall\ t \ge \hat{T}_g^U + t_b^+ - 1 \tag{20}$$

$$\sum_{k=t-\hat{T}_g^D+1}^{t} u_{k,g}^- \le N_g - u_{t,g} \quad \forall\ t \ge \hat{T}_g^D + t_b^+ - 1 \tag{21}$$

Logical constraint (19) represents the equation which guarantees the start-up variable $u_{t,g}^+$ and shut-down variable $u_{t,g}^-$ take the appropriate values when the generator units are online and offline [24]. Constraints (20) and (21) guarantee the minimum periods for which the units must be online and offline, where $\hat{T}_g^U$ and $\hat{T}_g^D$ represent the scaled number of hours that the generator units are online and offline, respectively. Assuming uniform sampling in demand blocks, $\hat{T}_g^U := \lceil T_g^{mu} \div \Delta_t \rceil$ and $\hat{T}_g^D := \lceil T_g^{md} \div \Delta_t \rceil$ where $\lceil \cdot \rceil$ denotes the ceiling function that gives as output the least integer equal or greater than the value of its argument. The generation limits are as follows ([24, 30]) $\forall b \in \Omega_B$, $\forall t \in \Omega_T^b$, $\forall g \in \Omega_G$

if $T_g^{mu} \ge 2$

$$\begin{aligned} 0 \le p_{t,g} + rsp_{t,g} + res_{t,g} \le \left(\overline{P}_g - p_g^{msg}\right) u_{t,g} \\ -\left(\overline{P}_g - SU_g\right) u_{t,g}^+ - \left(\overline{P}_g - \mathrm{SD}_g\right) u_{t+1,g}^- \end{aligned} \tag{22}$$

if $T_g^{mu} = 1$,

$$\begin{aligned} 0 \le p_{t,g} + rsp_{t,g} + res_{t,g} \le \left(\overline{P}_g - p_g^{msg}\right) u_{t,g} \\ -\left(\overline{P}_g - SU_g\right) u_{t,g}^+ - \max\left(SU_g - \mathrm{SD}_g, 0\right) u_{t+1,g}^- \end{aligned} \tag{23}$$

$$\begin{aligned} 0 \le p_{t,g} + rsp_{t,g} + res_{t,g} \le \left(\overline{P}_g - p_g^{msg}\right) u_{t,g} \\ -\max\left(\mathrm{SD}_g - SU_g, 0\right) u_{t,g}^+ - \left(\overline{P}_g - \mathrm{SD}_g\right) u_{t+1,g}^- \end{aligned} \tag{24}$$

where cyclic boundary conditions $u_{t_b^-,g}^- = u_{t_b^+,g}^-$ are enforced $\forall b \in \Omega_B$ and $\forall\ g \in \Omega_G$. The generation limit equations include the power output $p_{t,g}$, spinning reserve $res_{t,g}$ and frequency response $rsp_{t,g}$ contributions of the clustered units. Constraints (23) and (24) only apply for the subset of clustered generator units with $T_g^{mu} = 1$, while constraint (22) is for the subset of generators with $T_g^{mu} \ge 2$. The authors in Ref. [24] emphasise that constraint (22) is much tighter and compact than constraints (23) and (24). To impose that candidate generators can operate only if the necessary investment has taken place, we model linear constraints linking the operation of candidate generators g to the integer investment G_{n,g_T} [13]. In particular, the proposed constraints impose that the variables $u_{t,g}$, $u_{t,g}^+$, $u_{t,g}^-$ can assume non-zero values only if the cluster g has been built. For all $b \in \Omega_B$, $\forall t \in \Omega_T^b$ and $g \in \Omega_N \times \Omega_G^T$ the following constraints,

$$u_{t,g} \le G_{n,g_T},\ u_{t,g}^+ \le G_{n,g_T}, u_{t,g}^- \le G_{n,g_T}. \tag{25}$$

guarantee that aggregate generators can be active only if the relative investment occurs.

The operating initial conditions of the generator units at time t - 1, which considers the previous state of the units, are imposed in this model. The system's initial condition depends on the operating conditions at the end of the demand period, given each demand block represents a typical period in the year. The conditions are as follows:

$$u_{t_b^+,g} - u_{t_b^-,g} = u_{t_b^+,g}^+ - u_{t_b^+,g}^-, \tag{26}$$

$$\sum_{k=\hat{t}_b^- - \hat{T}_g^U+1+t}^{\hat{t}_b^-} u_{k,g}^+ + \sum_{k=\hat{t}_b^+}^{t} u_{k,g}^+ \le u_{t,g} \quad \forall\ \hat{t}_b^+ \le t \le \hat{T}_g^U + t_b^+ - 1 \tag{27}$$

$$\sum_{k=\hat{t}_b^- - \hat{T}_g^D+1+t}^{\hat{t}_b^-} u_{k,g}^- + \sum_{k=\hat{t}_b^+}^{t} u_{k,g}^- \le N_g - u_{t,g} \quad \forall\ t_b^+ \le t \le \hat{T}_g^D + t_b^+ - 1 \tag{28}$$

The total power produced by the cluster $g \in \Omega_N \times \Omega_G^T$ is expressed as the sum of two terms as follows:

$$P_{t,g} = p_g^{msg} u_{t,g} + p_{t,g} \quad \forall\ t, g. \tag{29}$$

The first term describes the unit's minimum stable generation and the second one is the additional generation output over the minimum. Total commitment, frequency response, spinning reserve and production output of the clustered units, which sums up the contributions from individual generator units, are given by

$$u_{t,g} = \sum_{i \in \Omega_I^g} \tilde{u}_{t,g,i} \quad \forall\ t, g \tag{30}$$

$$rsp_{t,g} = \sum_{i \in \Omega_I^g} r\tilde{s}p_{t,g,i} \quad \forall\ t, g \tag{31}$$

$$res_{t,g} = \sum_{i \in \Omega_I^g} r\tilde{e}s_{t,g,i} \quad \forall\ t, g \tag{32}$$

$$p_{t,g} = \sum_{i \in \Omega_I^g} \tilde{p}_{t,g,i} \quad \forall\ t, g \tag{33}$$

The computation of constraints (30)–(33) is based on the need to model the individual ramping constraints of generators in the clustered unit to avoid the overestimation of their ramping and reserve flexibility [16]. A commitment order in every cluster is enforced $\forall\ t, g$ to remove multiple equivalent solutions as follows:

$$\tilde{u}_{t,g,1} \le 1 \tag{34}$$

$$\tilde{u}_{t,g,i+1} \le \tilde{u}_{t,g,i} \quad \forall\ i = 2, \ldots, Ng - 1 \tag{35}$$

$$\tilde{u}_{t,g,N_g} \ge 0 \tag{36}$$

$$\begin{aligned} &\tilde{p}_{t,g,i+1} + r\tilde{s}p_{t,g,i+1} + r\tilde{e}s_{t,g,i+1} \le \\ &\quad \tilde{p}_{t,g,i} + r\tilde{s}p_{t,g,i} + r\tilde{e}s_{t,g,i} \quad \forall\ i = 1, \ldots, Ng - 1 \end{aligned} \tag{37}$$

Constraints (34) to (36) have been modelled according to Ref. [16] to ensure the successive order of commitment of the units starting from unit 1, while constraint (37) is introduced to ensure symmetries in the generators' model are removed and the production of individual units are limited. The model which properly estimates the start-up and shut-down capabilities for the individual generator units i is as shown in constraints (38)–(40) $\forall\ t, g, i = 1, \ldots, Ng$:

if $T_g^{mu} \ge 2$:

$$\begin{aligned} &\tilde{p}_{t,g,i} + r\tilde{s}p_{t,g,i} + r\tilde{e}s_{t,g,i} \le \left(SU_g - p_g^{msg}\right)\tilde{u}_{t,g,i} \\ &\quad + \left(\overline{P}_g - SU_g\right)\tilde{u}_{t-1,g,i} \quad \forall\ t, g, i = 1, \ldots, Ng \end{aligned} \tag{38}$$

$$\begin{aligned} &\tilde{p}_{t,g,i} + r\tilde{s}p_{t,g,i} + r\tilde{e}s_{t,g,i} \le \left(\mathrm{SD}_g - p_g^{msg}\right)\tilde{u}_{t,g,i} \\ &\quad + \left(\overline{P}_g - \mathrm{SD}_g\right)\tilde{u}_{t+1,g,i} \quad \forall\ t, g, i = 1, \ldots, Ng \end{aligned} \tag{39}$$

and if $T_g^{mu} = 1$:

$$\begin{aligned} &\tilde{p}_{t,g,i} + r\tilde{s}p_{t,g,i} + r\tilde{e}s_{t,g,i} \le \left(SU_g - \overline{P}_g + \mathrm{SD}_g - p_g^{msg}\right)\tilde{u}_{t,g,i} \\ &\quad + \left(\overline{P}_g - SU_g\right)\tilde{u}_{t-1,g,i} + \left(\overline{P}_g - \mathrm{SD}_g\right)\tilde{u}_{t+1,g,i} \end{aligned} \tag{40}$$

The ramping limits for the individual units are guaranteed with the following constraints $\forall\ t, g, i = 1, \ldots, Ng$:

$$\tilde{p}_{t,g,i} - \tilde{p}_{t-1,g,i} + r\tilde{s}p_{t,g,i} + r\tilde{e}s_{t,g,i} \le RU_g \Delta_t \tilde{u}_{t,g,i} \tag{41}$$

$$\tilde{p}_{t-1,g,i} - \tilde{p}_{t,g,i} \le RD_g \Delta_t \tilde{u}_{t-1,g,i} \tag{42}$$

In addition, the present model includes fast reserves for frequency response and spinning reserves. Thermal generators and storage devices can all contribute to the achievement of the system frequency response and reserve requirements $\forall b \in \Omega_B, \forall\ t \in \Omega_T^b$:

$$\begin{aligned} &\sum_{g \in \Omega_G} \sum_{i \in \Omega_I^g} r\tilde{s}p_{t,g,i} + \sum_{n \in \Omega_N} \Big(\sum_{es \in \Omega_S^E} \hat{\alpha}_{t,n,es}^{rsp} \\ &\quad \ge P_t^L - R_t^{slack} \end{aligned} \tag{43}$$

$$\begin{aligned} &\sum_{g \in \Omega_G} \sum_{i \in \Omega_I^g} r\tilde{e}s_{t,g,i} + \sum_{n \in \Omega_N} \left\{ \sum_{es \in \Omega_S^E} \hat{\alpha}_{t,n,es}^{res} \right\} \\ &\quad \ge Res_t^{\min} - R_t^{slack}. \end{aligned} \tag{44}$$

Constraints (43) and (44) ensure adequate contributions from the thermal generators and storage devices for meeting the minimum frequency response and spinning reserves, respectively, where the minimum reserves requirement are given by

$$Res_t^{\min} = 0.1 \left\{ \sum_{n \in \Omega_N} \left(d_{t,n} + \sum_{r \in \Omega_R} p_{t,n,r}^R \right) \right\} \tag{45}$$

The spinning reserve requirements depend on uncertainty or forecast error in intermittent generation and demand. All the generation and storage contributions $rsp_{t,g}$, $\hat{\alpha}_{t,n,es}^{res}$ and $\hat{\alpha}_{t,n,es}^{rsp}$ are subject to physical limitations $\forall b \in \Omega_B, \forall\ t \in \Omega_T^b, \forall\ es \in \Omega^S$

$$0 \le \hat{\alpha}_{t,n,es}^{rsp} \le \overline{Rsp}_{es} := P_L^{\max},\ 0 \le \hat{\alpha}_{t,n,es}^{res} \le \overline{Res}_{es} \tag{46}$$

$$\left(\hat{\alpha}_{t,n,es}^{res} + \hat{\alpha}_{t,n,es}^{rsp}\right) \le \hat{S}_{es}^{-} - h_{t,n,es}^{-} + h_{t,n,es}^{+} \tag{47}$$

$$\left(N_{es}^{rsp} \hat{\alpha}_{t,n,es}^{rsp} + N_{es}^{res} \hat{\alpha}_{t,n,es}^{res}\right) \le \tilde{h}_{t,n,es} \tag{48}$$

$$0 \le r\tilde{s}p_{t,g,i} \le \tilde{u}_{t,g,i} \overline{Rsp}_g \tag{49}$$

where $\overline{Rsp}_g$ and $\overline{Rsp}_{es}$ are the maximum frequency response capabilities of a generation unit in the cluster g and of storage es, respectively. The parameters N_{es}^{res} and N_{es}^{rsp} refer to the time, and storage s must provide the slow and fast response, respectively. The power output of intermittent sources satisfies, $\forall b \in \Omega_B$, $\forall t \in \Omega_T^b$, $\forall n \in \Omega_N$ and $\forall r \in \Omega_R$,

$$0 \le p_{t,n,r}^R \le \xi_{t,r,n}\left(R_{n,r} + R_{r,n}^0\right) \tag{50}$$

where $R_{n,r}$ is the capacity size (MW) of candidate renewable installations, $R_{r,n}^0$ represents the existing capacity and $\xi_r(t)$ is the performance factor of technology r at time t.

The carbon emissions of a thermal unit in the cluster g at time t can be modelled as a linear function of the generated power and the annual carbon limits as follows:

$$\sum_{b\in\Omega_B} w_b \left(\sum_{g\in\Omega_G} \sum_{t\in\Omega_T} \left(a_g^V \Delta_t \left(p_{t,g} + p_g^{msg} u_{t,g} \right) + a_g^{NL} u_{t,g} + a_g^{UP} u_{t,g}^+ \right) \right) \le \sum_{b\in\Omega_B} w_b \sum_{n\in\Omega_N} \sum_{t\in\Omega_T^b} \left(E^T d_{t,n} \right) \tag{51}$$

where a_g^V (kg/MWh) is the variable emission coefficient of the cluster g, a_g^{NL} $(kgCO_2)$ the no load emission coefficient and a_g^{UP} $(kgCO_2)$ the start-up load emission coefficient. The adopted UC formulation, presented in this section, combining constraints on the aggregates and single generators, ensures quality and faster solutions and reduces computational burden compared to using either classic clustered or binary UC formulation alone [16]. Apart from reducing computational burden, the proposed modelling technique accurately evaluates the flexibility provided by every single generator when considering frequency response constraints.

3.3 | Frequency response constraints

The proposed model, similar to [19], combines the new FR service, EFR, recently introduced by National Grid in Great Britain (GB), which should deliver responses within 1 s, together with primary frequency response services from available conventional generators delivered in less than 10 s. The analysis of the swing equation, describing the time evolution of frequency deviation after a generation outage, allows the identification of constraints guaranteeing the satisfaction of the dynamic frequency requirements. The swing Equation (52) describes the frequency dynamic as a function of the time τ immediately after a generation outage P_t^L occurs at time t [19]:

$$\frac{2H_t}{f_o}\frac{d\Delta f(\tau)}{d\tau} + D P_t^D \Delta f(\tau) = \sum_{es\in\Omega_S^E} EFR_{t,es}(\tau) + \sum_{g\in\Omega_G^T} PFR_{t,g}(\tau) - P_t^L \tag{52}$$

where

$$EFR_{t,es}(\tau) = \begin{cases} R_{t,es}^{ES}\tau/T^{es} & \text{if } \tau \le T^{es} \\ R_{t,es}^{ES} & \text{if } \tau > T^{es} \end{cases} \tag{53}$$

$$PFR_{t,g}(\tau) = \begin{cases} R_{t,g}^{G}\tau/T^{G} & \text{if } \tau \le T^{G} \\ R_{t,g}^{G} & \text{if } \tau > T^{G} \end{cases} \tag{54}$$

The largest power in-feed P_t^L satisfies $\forall b \in \Omega_B$, $\forall t \in \Omega_T^b$

$$\tilde{p}_{t,g,i} + p_g^{msg}\tilde{u}_{t,g,i} \le P_t^L \le P_L^{\max}, \quad \forall g \in \Omega_G, i = 1, \ldots, Ng \tag{55}$$

$$\Psi \le P_t^L \le P_L^{\max} \quad \forall\ r \in \Omega_R,\ \forall n \in \Omega_N \tag{56}$$

where Ψ is a parameter to be chosen by the planner to take into account other losses that are relevant, such as the loss of a wind farm of a certain size. The definition of P_t^L as a decision variable $\forall b \in \Omega_B$ and $\forall t \in \Omega_T^b$ is advantageous because dynamically choosing the largest power in-feed reduces the maximum potential RoCoF after a generator loss, as supported by [31]. This approach is more efficient than increasing the inertia levels in the system through the addition of synchronous generators, as it would not be a long-term economical solution, given the decreasing system inertia due to renewable integration.

The highest value for the RoCoF occurs at $\tau = 0$ and the RoCoF security constraint [19] at the instant of outage $\forall b \in \Omega_B$, $\forall t \in \Omega_T^b$ is

$$0 \le \frac{P_t^L f_0}{2H_t} \le \overline{RoCoF} \tag{57}$$

Note that condition (57) guarantees that $\Delta f(\tau)$ cannot become smaller than $\Delta f_{\max} = -0.8$ Hz before $\hat{\tau} = 0.8/RoCoF_{\max} = 1.6$s. This implies that a minimum of $\Delta f(\tau)$ occurring at values $\tau \le \hat{\tau}$ does not correspond to a critical situation. For this reason, we will consider only the minimum sitting in the interval $[T_{es}, T_g]$ since in our case studies $T_{es} < \hat{\tau}$.

The system inertia level after the largest generator loss is

$$H_t = \sum_{g\in\Omega_G} \sum_{i\in\Omega_I^g} H_g \overline{P}_g \tilde{u}_{t,g,i} - H_t^{Loss} \tag{58}$$

$$P_g^{\max,L} H_g^L \tilde{u}_{t,g,i} \le H_t^{Loss} \quad \forall g \in \Omega_G, \forall i \tag{59}$$

$$\delta \le H_t \tag{60}$$

where $P_g^{\max,L}$ is the size of the largest generator and δ is a constant parameter satisfying $0 < \delta \le \min_{g\in\Omega_G} H_g \overline{P}_g$. The condition in (59) ensures considering the most significant possible inertia level loss H_t^{Loss} at every time, while Equation (60) requires the existence of at least a conventional

generator online. Constraint (60) models the minimum requirement for system inertia, a key consideration proposed in a system with a high penetration of variable renewable technologies [32, 33].

To ensure the achievement of quasi-steady state security, we impose the following constraint $\forall b \in \Omega_B, \forall t \in \Omega_T^b$

$$\frac{P_t^L - R_t^{ES} - R_t^G}{D P_t^D} \leq \Delta f_{\max}^{ss}, \tag{61}$$

where the total EFR, R_t^{ES}, satisfies

$$R_t^{ES} := \sum_{es \in \Omega_S^E} R_{t,es}^{ES} = \sum_{n \in \Omega_N} \sum_{es \in \Omega_S^E} \hat{\omega}_{t,n,es}^{rsp} \tag{62}$$

where

$$\hat{\omega}_{t,n,es}^{rsp} \leq \hat{\alpha}_{t,n,es}^{rsp} \tag{63}$$

The introduction of $\hat{\omega}_{t,n,es}^{rsp}$ allows for flexibility in the actual amount of frequency response that can be allocated by energy storage, where $\hat{\alpha}_{t,n,es}^{rsp}$ is the maximum allocated.

The total PFR, R_t^G, is such that

$$R_t^G := \sum_{g \in \Omega_G} R_{t,g}^G = \sum_{g \in \Omega_G} \sum_{i \in \Omega_I^g} \tilde{rsp}_{t,g,i} \leq \sum_{g \in \Omega_G} \sum_{i \in \Omega_I^g} \overline{Rsp}_g \tilde{u}_{t,g,i} \tag{64}$$

it is also required:

$$R_t^G \geq \underline{R}^G := \min_{g \in \Omega_G} \overline{RSP}_g \tag{65}$$

Based on the analysis performed in Ref. [19], the following quadratic expression accounts for the frequency nadir requirements.

$$\left(\frac{H_t}{f_0} - \frac{R_t^{ES} T^{es}}{4 \Delta f_{\max}}\right) R_t^G \geq \frac{\left(P_t^L - R_t^{ES}\right)^2 T^G}{4 \Delta f_{\max}} - \frac{\left(P_t^L - R_t^{ES}\right) T^G D}{4} P_t^D \tag{66}$$

Note that constraint (66) takes into account the effect of damping, and its good approximation properties are discussed in Ref. [19].

Moreover, since the nadir frequency occurs at time $t' \in [0, T_g]$, the following constraints have been included $\forall b \in \Omega_B, \forall t \in \Omega_T^b$,

$$P_t^L - R_t^{ES} - D P_t^D \left|\Delta f_{nadir}\right| \geq 0 \tag{67}$$

$$P_t^L - R_t^{ES} - D P_t^D \left|\Delta f_{nadir}\right| \leq R_t^G \tag{68}$$

to ensure the requirements are met within the response time of the frequency response services. The quadratic expression for the nadir constraint (66) is non-convex. Consequently, the resulting model is a mixed integer quadratic programming (MIQP) problem. The mixed integer model, including the non-convex quadratic constraint, is efficiently solvable to global optimality by applying McCormick relaxations and spatial techniques as implemented in the Gurobi solver (starting from version 9.1.2) to a MIPGap of 0.1% [25]. Constraint 66 includes three non-linear terms: Products of continuous and binary/Integer variables $H_t R_t^G$ and $R_t^{ES} R_t^G$ as well as the quadratic term $\left(P_t^L - R_t^{ES}\right)^2$. McCormick lower and upper envelopes are applied to the products using auxiliary variables to linearise the bilinear terms in the nadir constraints [25]. Such that $H_t R_t^G$ is

$$H_{t,l} R_t^G + R_{t,l}^G H_t \leq H_{t,l} R_{t,l}^G \tag{69}$$

$$H_{t,u} R_t^G + R_{t,u}^G H_t \leq H_{t,u} R_{t,u}^G \tag{70}$$

$$H_{t,u} R_t^G + R_{t,l}^G H_t \leq H_{t,u} R_{t,l}^G \tag{71}$$

$$H_{t,l} R_t^G + R_{t,u}^G H_t \leq H_{t,l} R_{t,u}^G \tag{72}$$

where $H_{t,l}, H_{t,u}, R_{t,l}^G, R_{t,u}^G$ is the lower and upper bound of $H_t R_t^G$ respectively. The other products are linearised in a similar manner and added to the model. The linearised coefficients and RHS of the McCormick constraints depend on variables' local bounds, which, once changed, update the LP coefficients and RHS. The above constraints are then added via spatial branching techniques as locally valid cuts [25]. The spatial branching technique minimises the McCormick volume as much as possible [25]. The tighter McCormick relaxations replace weaker, more global ones, at local nodes leading to fewer simplex iterations to support the solution of the transformed MILP problem. In addition, compared to other solvers, Gurobi delivers a globally valid lower bound on the optimal objective value by exploring the entire search space and with enough time, through the tolerance, finds a globally optimal solution [25].

4 | PROBLEM FORMULATION FOR MODEL WITHOUT SCHEDULING CONSTRAINTS

In highlighting the benefits of detailed scheduling constraints in the proposed planning framework, this subsection presents a similar system design but with the classic clustered integer UC formulations often adopted in research today. The planning framework was adapted to integrate a deterministic formulation of the mixed integer UC constraints proposed by the authors in Refs. [19, 34]. The design mainly excludes the ramping and commitment constraints formulations for the

single generators proposed in Section 3.1, Equations (30)–(42), which evaluates the flexibility of individual generators in the optimisation model. The formulation serves as a good baseline for comparison because it also includes the inertia-dependent post-fault frequency response requirements being adapted in the proposed model in the previous section. With the same constraints in Section 3.1 implemented, especially for other technologies such as storage, hydrogen electrolysers, blue hydrogen, and renewable technologies, this section presents only key parts of the model that were modified according to where the clustered UC variable, N^{up}_{t,n,g_T}, applies.

The problem formulation for the model without scheduling constraints is as follows:

$$V^O(x,\rho) := \sum_{b\in\Omega_B} w_b \sum_{t\in\Omega^b_T} \left\{ \tau_t \left[\sum_{g\in\Omega_G} c^G_g\left(P_{t,g}\right) + \sum_{n\in\Omega_N} \left[\sigma^d_{t,n} + \sum_{s\in\Omega^n_S} \left(c^+_s h^+_{t,s} + c^-_s h^-_{t,s} \right) \right] \right] + \Upsilon R^{slack}_t + \sum_{g\in\Omega_G} c_{res} res_{t,g} + \sum_{g\in\Omega_G} c_{rsp} rsp_{t,g} \right\} \tag{73}$$

It is important to note that based on the model formulation in Refs. [19, 34], the operation cost objective function $V^O(x,\rho)$ in constraint (73) excludes the start-up and shut-down costs. The generation limits [24, 30] for this case, which excludes detailed scheduling constraints, are as follows: $\forall b \in \Omega_B$, $\forall t \in \Omega^b_T$, $\forall g \in \Omega_G := \Omega_N \times \Omega^T_G$

$$0 \le P_{t,g} + rsp_{t,g} + res_{t,g} \le \left(\overline{P}_g N^{up}_{t,n,g_T}\right) \tag{74}$$

The power output, frequency response and spinning reserve contributions of the clustered units are bounded by their maximum total amount of power output based on the number of generators online N^{up}_{t,n,g_T} per time. We propose new linear constraints linking the operation of candidate generators g_T to the integer investment G_{n,g_T} to impose that a candidate generation unit can operate only if the necessary investment has taken place. In particular, the proposed constraints impose that the variables N^{up}_{t,n,g_T} can assume a non-zero value only if the generator g_T has been built. For all $b \in \Omega_B$, $\forall t \in \Omega^b_T$ and $g_T \in \Omega^T_G$ the following constraints,

$$N^{up}_{t,n,g_T} \le G_{n,g_T} \tag{75}$$

guarantee that a candidate generator can be active only if the relative investment has taken place. The ramp-up/down constraints for the clustered units are as follows: $\forall b \in \Omega_B$, $\forall t \in \Omega^b_T - \left\{t^+_b\right\}$, $\forall g \in \Omega_G$

$$P_{t,g} - P_{t-1,g} + rsp_{t,g} + res_{t,g} \le RU_g \tau_t N^{up}_{t,n,g_T} \tag{76}$$

$$P_{t-1,g} - P_{t,g} \le RD_g \tau_t N^{up}_{t-1,n,g_T} \tag{77}$$

The thermal generators are also modelled to satisfy minimum up/down times and logical constraints, similar to constraints (19 − 21). However. in this case, $u_{t,g}$ is replaced with N^{up}_{t,n,g_T}. All the frequency response contribution from the clustered generation units $rsp_{t,g}$ are subject to physical limitations $\forall b \in \Omega_B$, $\forall t \in \Omega^b_T$, as in

$$0 \le rsp_{t,g} \le \overline{Rsp}_g N^{up}_{t,n,g_T} \tag{78}$$

The largest power in-feed P^L_t at time t is implemented such that

$$\frac{P_{t,g}}{N^{up}_{t,n,g_T}} \le P^L_t \le P^{\max}_L, \quad \forall g \in \Omega_G, i = 1,\ldots,Ng \tag{79}$$

This expression provides a non-linear expression of the decision variable P^L_t, given the need to optimise the largest loss of a single power production unit [19]. The expression was linearised using Big-M formulation and McCormick relaxation techniques, given that N^{up}_{t,n,g_T} is an integer decision variable [19]. The RoCoF, nadir and steady-state security constraints used in this formulation are similar to constraints (57), (61) and (66).

However, the system inertia level after the largest generator loss is

$$H_t = \sum_{g\in\Omega_G} H_g \overline{P}_g N^{up}_{t,n,g} - P^{\max}_L H_L. \tag{80}$$

These constraints were used to carry out further studies.

5 | METHODS AND TEST SYSTEM

The proposed model outlined above is applied to a single-node system to determine the generation (conventional, renewable and storage) mix for meeting system's different energy, frequency response and reserve requirements. The co-optimisation of investment and operation constraints led to a large number of constraints and variables in the model, shown in Table 1.

TABLE 1 Model components.

Model Components	Total Constraints	Quadratic Constraints	Bilinear Constraints
Number	4226902	672	1344
Total Variables	Continuous Variables	Integer Variables	Binary Variables
1915225	1436757	478468	470400

TABLE 2 Candidate generator data.

Type	p_g^{msg} (MW)	$\overline{P}_g$ (MW)	κ_g^G ($/yr)	c_g^G ($/MWh)	c_g^{su} ($)
HT	500	500	54813.2.9	38	30780
Nc	1440	1800	530582.0	6	56710

TABLE 3 Technical thermal generators data.

Type	H_g (s)	$\overline{Rsp}_g$ (MW)	T_g^{md} (h)	T_g^{mu} (h)	RU_g/RD_g (%$\overline{P}_g$/minute)
HT	4	85	4	4	60
Nc	5	0	4	4	1

TABLE 4 Candidate renewable generator data.

No.	$R_{n,r}$ (MW)	κ_r^R ($/yr)
Wind	6000	57565.77
Solar	1500	50261.2

TABLE 5 Candidate storage data.

$\overline{\eta}_s$	$\overline{h}_s$ (MWh)	ρ_s (MW)	κ_s^H ($/yr)	c_s ($/MW)	N_s^{res} (h)	N_s^{rsp} (h)
200	50	0.85	7650.76	5	4	0.5

The numerical complexity of the problem and the large number of constraints and variables led to the decision to carry out this study first on a single-node system. The system does not assume any existing conventional generator types. Two candidate conventional generation technologies (H_2CCGT (HT), Nuclear (NC), generators) [28, 35] investments are considered on a single node, with their parameters shown in Tables 2 and 3.

Also, battery storage, renewable solar and wind generator technologies, electrolysers and hydrogen storage are part of the investment portfolio. The used renewable parameters are shown in Table 4.

The four seasons' (winter, spring, summer and autumn) wind and solar performance level factors have been extracted from GB historical data. Table 5 reports technical details for the storage. The Lithium Ion battery storage technology is modelled to have the capability of EFR service provision delivered within $T_s = 0.5$ s with $\overline{Rsp}_s = \overline{Res}_s$. The conventional generators provide PFR within $T_g = 10$ s. Other parameters include $D = 0.5\%/\text{Hz}$ and $P_L^{\max} = 1800$ MW. The dynamic frequency requirements are set as in Ref. [19].

The parameters for the blue and green hydrogen production (gas-heated reformers with carbon capture storage, GHR-CCS, and electrolysers, respectively) [28], as well as storage technologies, are shown in Table 6.

The hydrogen storage duration is 6 h, while the conversion efficiency of H_2CCGT, η_{h2}, is 58.8% [28]. The marginal cost of GHR-CCS is higher, compared to electrolysers, due to the consideration of the CCS for decarbonising the hydrogen fuel produced.

TABLE 6 Hydrogen production and storage technologies data.

Technology (o)	κ_o^H ($/yr)	c_o ($/MW)	η_o (%)
Electrolyser	36066.94	2.1	82%
Hydrogen storage	520.05	0.149	99.67%
GHR-CCS	37222.43	61	61%

Demand profiles used on this system are based on representative historical typical days data from the GB system. Four different week-long demand block profiles, representing all seasons of the year (winter, spring, summer and autumn) are considered, and the system's annual peak (electricity) demand is 71 GW, which totals to 167.9 GW after including heat demand in the system [35]. This paper assumes that the heat sector will be decarbonised through electrification using heat pumps. Considering hydrogen demand, the amount of hydrogen is estimated by the model. However, the hydrogen production and storage modelling also considers an additional 123 TWh hydrogen demand, with a profile modelled as flat, based-industrial processes in a 2050 GB net-zero scenario [1, 35].

The model was implemented in PYOMO [36, 37] and solved with the Gurobi Optimiser 10.0.0[25] on a High-Performance computer with linux64, 128 physical cores, and 256 logical processors, using up to 16 threads.

6 | RESULTS

Recalling that the research goal is to determine the influence of frequency response and detailed modelling of operational constraints in an integrated planning framework, a series of scenario studies were considered on the test system. The system settings common to all scenarios included

- The annual CO_2 emissions target, E^T, was set to 0 kg/MWh, representing the net-zero system.
- The generator scheduling constraints included the on/off status, minimum up/down time and start-up/shut-down trajectories of conventional generators.
- Battery storage was also modelled to provide flexibility in terms of energy arbitrage, spinning reserves and primary frequency response.
- The model was run with an hourly temporal resolution for one typical week per seasonal block at the operational level to determine the optimal power generation portfolio.

The obtained optimal generation mixes are analysed hereafter under different scenarios.

6.1 | Scenario description

This subsection analyses the optimal technology portfolio mix with and without the modelling of detailed scheduling

constraints for synchronous generators as constructed in Sections IV and VI, respectively. The case studies discussed in the section analyse the value of detailed scheduling constraints for synchronous generators such as Hydrogen CCGT (H_2CCGT) fuelled by both blue and green hydrogen sources and moderately flexible nuclear plants (minimum stable generation set to 80% of its maximum capacity). Additional power generation technologies used in this scenario include renewable technologies (wind and solar plants). H_2CCGT, nuclear plants, and battery storage were modelled to provide spinning reserves, while primary frequency response (PFR) constraints were mostly delivered by battery storage and H_2CCGT.

This subsection also assesses the optimal technology portfolio mix considering frequency security constraints. We compare the optimal mix with and without frequency response requirements. Tables 7 and 8 show the system's costs (IC, OC, Total costs (TC) in billion (bn) pounds/year) for the scenarios with and without detailed scheduling constraints, respectively. In both scenarios, similar studies on the impact of the frequency response constraints in the model were carried out and reported.

6.1.1 | Value of modelling detailed scheduling constraints

The value of modelling detailed scheduling constraints will be assessed by comparing the system cost of Case A and Case E reported in Tables 7 and 8, respectively. The system cost in Table 7 includes detailed scheduling constraints, while Table 8 do not have detailed scheduling constraints. Case A, in Table 7 reports a higher systems cost (difference of \$4.56bn/yr) based on higher investment and operation costs compared to Case E. A smaller difference (\$73 million/yr) in the investment cost is observed compared to the difference in operation costs (\$3.9bn/yr), and the composition of the investment cost per technology is shown in Figure 1. Case E's almost similar investment portfolio reveals higher investment in wind plants, battery storage and hydrogen storage compared to Case A.

Figures 2a–d emphasise the differences between the capacity mixes and highlights reduced investment in blue and green hydrogen sources related to the reduction observed in H_2CCGT plants in Case E.

In a bid to understand the higher operation costs observed in Case A, the impacts of the detailed scheduling constraints are further assessed by fixing the technology investment solution of Case E as inputs for Case A. The simulation resulted in a total systems cost of \$476.14bn/yr, with the investment cost at \$27.75bn/yr and operation costs at \$443.33bn/yr, based on demand curtailments. The results reported in Figure 3 show the demand curtailment costs (\$443.33bn/yr) and additional operation costs (\$442.70bn/yr) to the system for meeting the demand if technology investments were based on the model outputs without detailed scheduling constraints. The high curtailment cost was due to an annual demand

TABLE 7 Annual systems cost for the Blue & Green hydrogen case with detailed scheduling constraints (Case A –All FR constraints included, Case B –Nadir constraints excluded, Case C –Nadir & Rocof constraints excluded, Case D –All FR constraints excluded).

Type	*CaseA*	*CaseB*	*CaseC*	*CaseD*
IC(\$bn/yr)	28.47	28.39	27.42	27.33
OC(\$bn/yr)	5.69	5.77	1.60	1.44
TC(\$bn/yr)	34.16	34.16	29.01	28.77

TABLE 8 Annual systems cost for the Blue & Green hydrogen case without detailed scheduling constraints (Case E –All FR constraints included, Case F –Nadir constraints excluded, Case G –Nadir & RoCoF constraints excluded, Case H –All FR constraints excluded).

Type	*CaseE*	*CaseF*	*CaseG*	*CaseH*
IC(\$bn/yr)	27.74	27.75	27.76	27.73
OC(\$bn/yr)	1.84	1.83	1.36	1.32
TC(\$bn/yr)	29.59	29.59	29.12	29.05

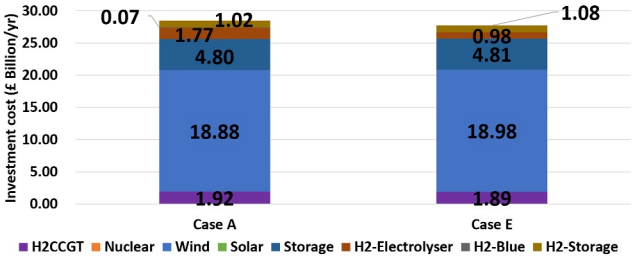

FIGURE 1 Investment cost per technology (Case A –Model with detailed scheduling constraints, Case E –model without detailed scheduling constraints).

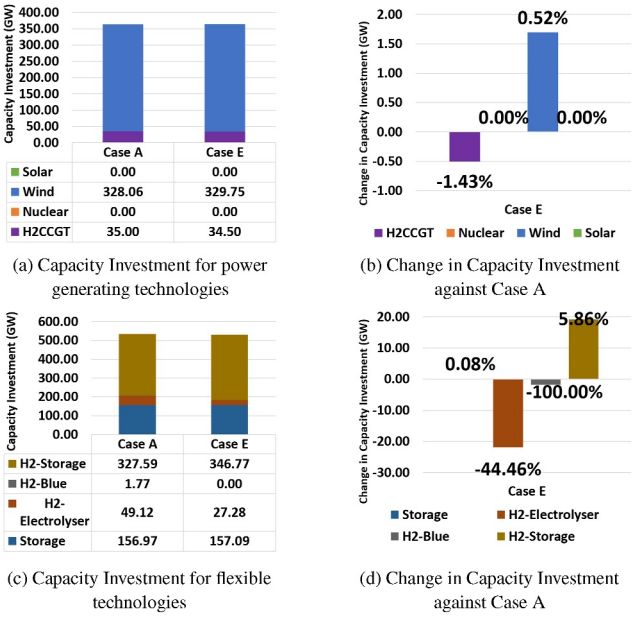

(a) Capacity Investment for power generating technologies

(b) Change in Capacity Investment against Case A

(c) Capacity Investment for flexible technologies

(d) Change in Capacity Investment against Case A

FIGURE 2 Capacity Investment of technologies for Blue –Green hydrogen case with versus without detailed scheduling constraints (Case A –Model with detailed scheduling constraints, Case E –model without detailed scheduling constraints).

curtailment of 14.78 TWh and its high price ($30,000/MWh), shown in Figures 4a,b. The Figure also highlights that most of the curtailment occurs in winter during periods of significant variations in net demand when ramping constraints are critical. In particular, Figure 4b shows that the H_2CCGT technologies did not ramp quickly enough during low wind and steep changes in net demand. The curtailment costs also led to a considerable change in operation costs observed in Figure 3. This disparity shows that even if the difference in system mix and cost is small, their ability to serve demand and satisfy constraints is very different.

6.1.2 | Value of modelling frequency security constraints

Cases B–C in Table 7 and Cases F–H in Table 8 report the optimised costs with and without scheduling constraints under different assumptions on the frequency response requirements. In particular, Cases B and F neglect the nadir constraints (66), Cases C and G do not include nadir and ROCOF constraints (but the constraints on the system inertia and largest generator loss are present in the model) and Cases D and H exclude all the frequency response constraints are excluded. The systems' costs for Cases A and B reported in Table 7 are similar, but the operation and IC differ. In Case B, which excludes the nadir constraints, the operation cost decreased by 1.39% and the investment cost increased by 0.28% compared to Case A, as shown in Figure 5. However, removing both the nadir and ROCOF constraints in Case C led to a 71.94% and 3.69% decrease in operations and IC, respectively. In Case C, the system inertia constraints 59 were included in the model. The inertia constraints are excluded in Case D, which led to a 74.61% and 4.01% decrease in operation and IC, respectively. The differences in the systems cost account for the additional flexibility needed for system security and stability [19].

Figure 5 also shows how the PFR constraints impact the solution when neglecting the detailed modelling of the scheduling constraints, using Case A as the base case. The removal of the PFR constraints in the manner described above shows a greater reduction in systems cost, especially the operation costs, between Cases B–D compared to Cases F–H without detailed scheduling constraints in Figure 5. However, very small changes are seen when assessing the impact of the frequency response constraints on the IC between Cases E–H. These minor differences in Cases E–H emphasise the value of the detailed modelling of the scheduling constraints for identifying the actual impact of the frequency constraints.

Figure 6 shows the system costs if the optimal investment mix obtained in Case D, which neglects frequency response constraints, is used in Cases A–C. The demand curtailment costs and change in OC with and without nadir constraints show similar high-cost effects of $341.35bn/yr and $340.7bn/yr, respectively. The high system costs in Cases A and B show the criticality of including the ROCOF and nadir constraints in a system with unlimited EFR from battery storage [23]. However, the demand curtailment costs and change in operations costs are much lower for Case C, where nadir and ROCOF constraints have been excluded. Figure 7 shows in

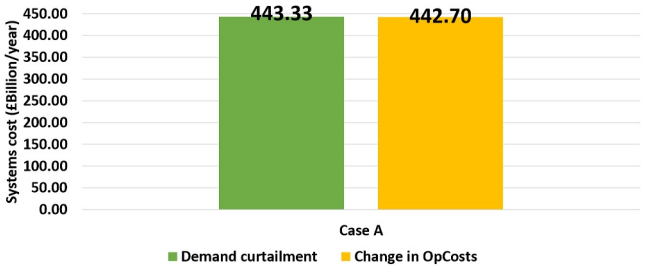

FIGURE 3 Demand curtailment & change in Operational cost for a fixed investment solution (Case A –Model with detailed scheduling constraints).

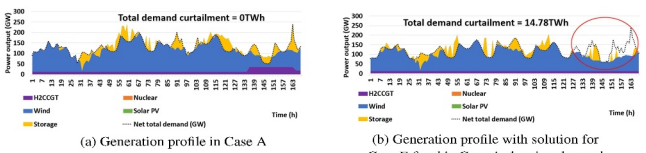

(a) Generation profile in Case A

(b) Generation profile with solution for Case E fixed in Case A showing demand curtailment

FIGURE 4 Generation profile for a typical winter week (Case A – Model with detailed scheduling constraints, Case E –model without detailed scheduling constraints).

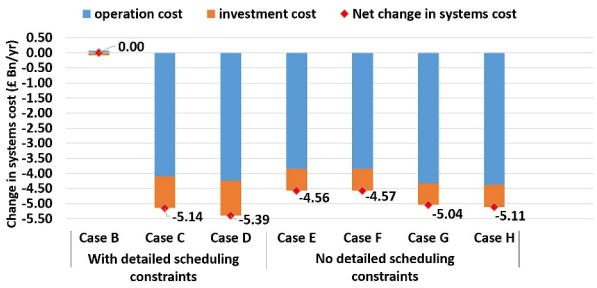

FIGURE 5 Change in systems cost for Blue & Green hydrogen case with versus without detailed scheduling constraints with respect to Case A (Case A –All FR constraints included, Case B –Nadir constraints excluded, Case C –Nadir & Rocof constraints excluded, Case D –All FR constraints excluded, Case E –All FR constraints included, Case F –Nadir constraints excluded, Case G –Nadir & RoCoF constraints excluded, Case H –All FR constraints excluded).

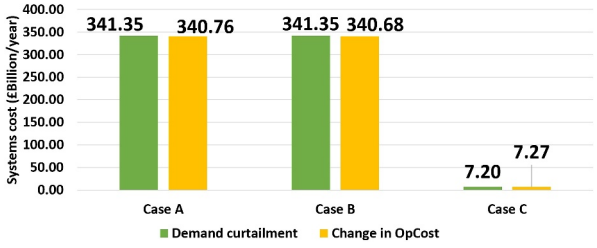

FIGURE 6 Demand curtailment & change in Operating costs using Case D solution (Case A –All FR constraints included, Case B –Nadir constraints excluded, Case C –Nadir & Rocof constraints excluded, Case D –All FR constraints excluded).

detail the season demand curtailment occurs, which was mostly in the winter period, as previously described.

The impact of excluding the PFR constraints on the power generation and flexible technologies capacity investment mix with and without detailed scheduling constraints is shown in Figure 8. Figure 8 shows the changes in the power generation capacity mix (wind, nuclear and H_2CCGT) for Case A of cases with detailed scheduling constraints and without detailed scheduling constraints. Figure 8 also shows changes in flexible technologies such as battery storage, H_2-storage Blue, and green (electrolysers) hydrogen fuel sources. In Case B of Figure 8, there is a 0.8% decrease in wind capacity and a 1.43% increase in H_2CCGT capacity. There is a corresponding increase in hydrogen storage, blue and green hydrogen fuel with the increase in H_2CCGT plant capacity, while battery storage also increased slightly, as observed in Figure 8. However, excluding the ROCOF constraints in addition to the nadir constraints, Case C in Figure 8, resulted in a further decrease in wind plant capacity by 3.19% and a further increase in H_2CCGT capacity by 5.71%. On the contrary, it can be observed in Figure 8 that the increase in H_2CCGT was matched with a decrease in blue and green hydrogen fuel but an increase in battery and hydrogen storage, as observed.

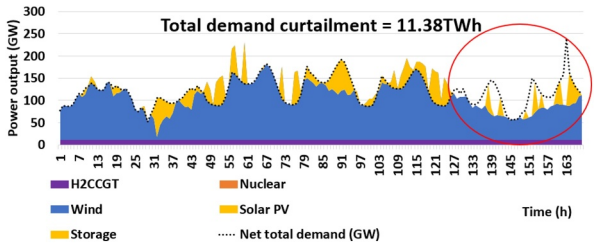

FIGURE 7 Generation profile in Case A for a typical winter week when Case D investment solution is fixed in Case A and Case C (Case A –All FR constraints included, Case D –All FR constraints excluded).

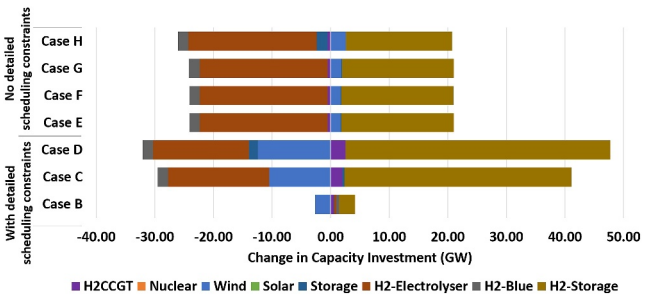

FIGURE 8 Change in capacity Investment of power and flexible generating technologies for Blue & Green hydrogen case with detailed scheduling constraints (Case A –All FR constraints included, Case B –Nadir constraints excluded, Case C –Nadir & Rocof constraints excluded, Case D –All FR constraints excluded, Case E –All FR constraints included, Case F –Nadir constraints excluded, Case G –Nadir & RoCoF constraints excluded, Case H –All FR constraints excluded).

An analysis of the annual generation profiles for Case C during the winter and spring week (Figure 9a,b) shows that H_2CCGT plants operate as peaking plants during critical periods of low wind generation and for a relatively short time (one or 2 days). The supply of large demand for short periods by H_2CCGT plants in a system with lower wind capacity, observed in Case C, compared to Cases A and B explains the increased investment in H_2CCGT and the further decrease in blue and green hydrogen, where H_2CCGT provided both the baseload and part of the peak generation. Also, using the optimal investment mix obtained by neglecting the RoCoF constraints with RoCoF limitations reports a demand curtailment of 11.81 TWh and consequently high costs of $354.39bn/yr.

Such demand curtailment represents the inadequacy of resource investments when nadir or RoCoF constraints are not considered in the planning phase. The changes in the technology investment mix in Case D, where all PFR security and inertia constraints are excluded, are similar to Case C but higher in percentage. The inadequacy of the technology investment mix obtained in Case D is highlighted in Figure 7, which reports substantial demand curtailment when frequency limitations must be satisfied.

The percentage changes observed in Cases E–H alternated such that investments in wind plants increased by 0.52% and H_2CCGT plant decreased by 1.43% based on excluding the detailed scheduling constraints. However, when comparing changes observed in Cases E–H in Figure 8 with changes in Cases A–D, the effect on the optimal mix induced by the frequency constraints is more evident considering detailed scheduling constraints. The investment capacity of wind and

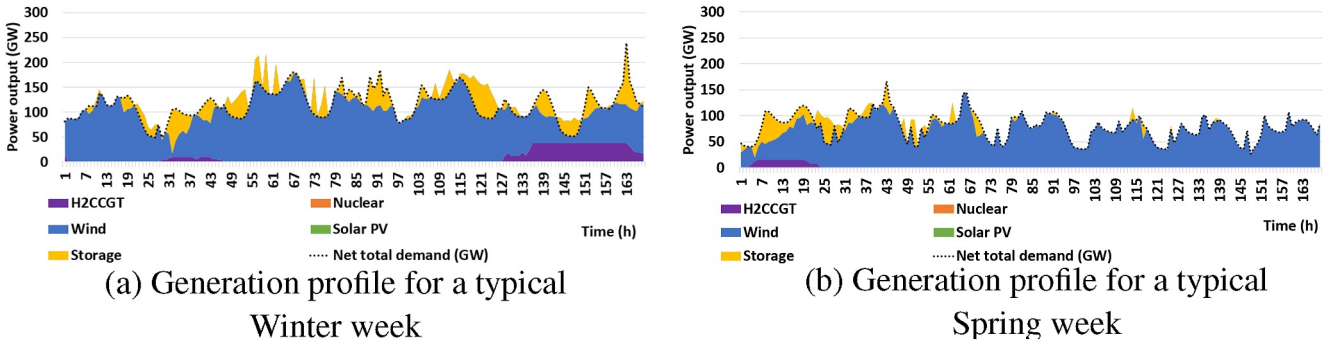

FIGURE 9 Generation profile in typical winter and spring week for Case C (Case C –Model with detailed scheduling constraints [Nadir & Rocof constraints excluded]).

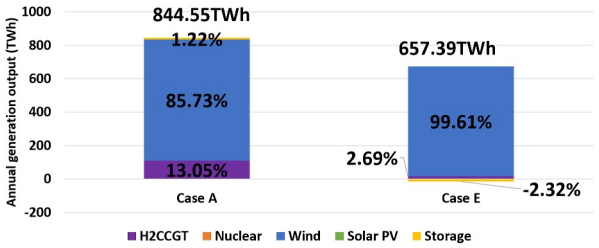

FIGURE 10 Share of Annual generation output (Case A –Model with detailed scheduling constraints, Case E –model without detailed scheduling constraints).

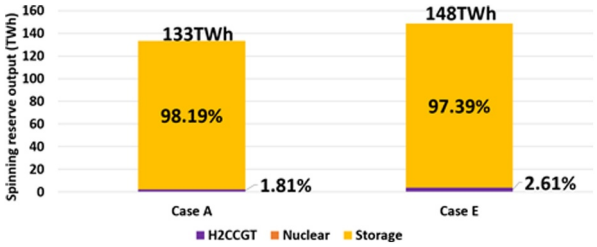

FIGURE 11 Share of Annual Spinning Reserve portfolio (Case A –Model with detailed scheduling constraints, Case E –model without detailed scheduling constraints).

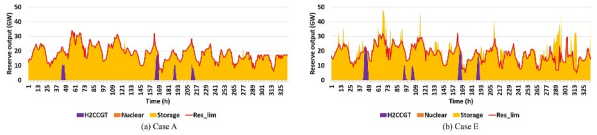

FIGURE 12 Spinning Reserve profile for a typical combined winter and spring week (Case A –Model with detailed scheduling constraints, Case E –model without detailed scheduling constraints).

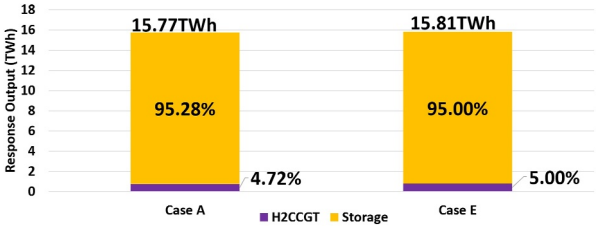

FIGURE 13 Share of Annual PFR portfolio (Case A –Model with detailed scheduling constraints, Case E –model without detailed scheduling constraints).

H_2CCGT plants are similar in Cases E–G. The most significant change in the scenarios without detailed scheduling constraints was the 0.79% change in wind plants observed in Case H when all the frequency security constraints were excluded from the model. Figure 8 also shows that for Cases E–H there is a corresponding increase in hydrogen storage capacity, while blue and green hydrogen fuel capacity decreases with the observed reduction in H_2CCGT plant capacity. However, there are no significant changes from excluding the frequency response constraints named in Cases F–H. Similar to Case D, the greatest decrease in battery storage is observed in Case H when the frequency response constraints are excluded.

Figure 10 shows the share of annual generation output for the installed technologies when detailed modelling is included (Case A) and excluded (Case E), based on the net demand on the system. The total generation output in Case A is 844.55 TWh, while Case E is 657.39 TWh. Even though the same system demand was used in both cases, the variation in their total generation output is mainly due to the flexible energy demand from the electrolysers used for hydrogen production. This flexible demand from the electrolyser is higher in Case A (13.05%), where the contribution from H_2CCGT to generation output is higher compared to Case E (2.69%). The high contribution of H_2CCGT in Case A is due to the detailed scheduling constraints, which depict the actual requirement of flexible generation on the system. However, wind plants deliver the highest percentage of annual generation output in both cases. Battery storage also contributes to the energy supply in both cases. In Case A, the charge–discharge activity of battery storage was summed and resulted in a net contribution of 1.22%, discharging more times than it charges. Whereas in Case E, the net contribution of battery storage is −2.32%, charging more times than it discharges.

Figures 11 and 13 compare the spinning reserve and the primary frequency response provision mix in Case A and Case E. In particular, Figure 11 shows that H_2CCGT and battery storage technology meet all the spinning reserves requirements, with batteries having the largest share. Given that the reserve requirement, $Res_t^{\min}$, is calculated as a percentage of system demand and renewable generation per time, the reserve requirement in Case E (148 TWh) is higher compared to Case A (133 TWh) due to higher investment in wind plant capacity observed in Figure 8. As a result, Case E shows a higher proportion of battery storage usage and H_2CCGT, respectively, for spinning reserve provision compared to Case A. Figure 12 provides further explanation for the results observed as it depicts the hourly scheduling of reserves in Cases A and E. The results show that in Case E, the technologies, especially storage, are scheduled in excess for reserves provision compared to Case A. The detailed modelling of the scheduling constraints eliminates the overestimation of reserves from different technologies.

A comparison of the Primary frequency reserve (PFR) portfolio in Figure 13 shows Case A and Case E are almost similar (circa. 16 TWh) based on the requirement estimated from the size of the largest generator loss $\left(P_t^L\right)$. In both cases, battery storage mostly provided a frequency response, given its enhanced and faster frequency response capability compared to H_2CCGT. However, the contribution of H_2CCGT capacity in Case E (0.79 TWh) was slightly higher compared to Case A (0.74 TWh). The higher availability of H_2CCGT in Case E can be linked to the reduced use of H_2CCGT for meeting energy demand, as observed in Figure 10.

7 | DISCUSSION

Energy system models, especially investment planning models, are required for decision-making and to provide insights to energy stakeholders on key technologies valuable for achieving

energy transition and decarbonisation targets. The proposed novel formulation and the case studies emphasise the importance of using an enhanced whole system model, which includes frequency requirements and detailed operational dynamics to support decision-making by policymakers, systems operators, utilities and investors.

The results of modelling detailed scheduling constraints in the proposed planning framework demonstrate that such modelling significantly impacts investment outcomes. The system cost increases to allow the system to edge against frequency variations. Specifically, the modelling ensured an appropriate estimation of the capacity of technologies needed to support the required system flexibility in a low-carbon future, and these were seen in the total capacity requirements for reserves and frequency response [32]. The changes observed were increased investment capacity in H_2CCGT plants, as well as blue and green hydrogen production technologies needed to fulfil the energy requirements in a net-zero system, compared to a model without the detailed representation of the scheduling constraints. Despite an observed reduction in investments in wind plants, the investments in these hydrogen technologies are also required to support the integration of renewable technologies, especially for managing periods of variable and low renewable generation [2]. Investments in battery and hydrogen storage capacity are directly related to investments in renewable technologies, such as the reduction in wind plants, which reduced the amount of storage capacity required to support the technology [38]. The significance of these changes is that high curtailment costs of up to \$443.33bn/yr were avoided when capacity planning was done using the outcomes of a model excluding the detailed modelling of UC constraints and the ramping capability of individual generators units in a cluster.

Similarly, modelling the different frequency security constraints in an investment planning framework aids system operators in accurately estimating investments in flexible technologies needed to support the system during a frequency round trip [10]. By layering frequency security constraints on the detailed scheduling constraints in the model, it was demonstrated that modelling frequency constraints support the integration of renewable technologies into the system, leading to increased investments in wind plant capacity. These changes were evident because of the ramping capability of individual generation units captured in the model. It was also realised that compared to a model without any of the frequency response constraints, the reduced capacity of H_2CCGT and hydrogen storage technologies are actually needed for supporting the system's flexibility. In addition, it was demonstrated that increased investment in battery storage was required to manage the frequency changes in the system based on its fast response. Considering nadir constraints and requirements at the planning level contributes to driving better investment decisions for managing near under-frequency load shedding situations. As shown in the case study, not considering nadir constraints at the planning level can cause very high curtailment costs of up to \$340bn/yr, no security of supply and reduced demand-supply balancing.

Even though the model can integrate a dynamic power in-feed loss, this study assumed the loss of the largest generator, which is a nuclear plant included in the technology mix. The sensitivity analysis on a dynamic power in-feed loss which could vary from the actual power output of a power production unit to the maximum power output of the largest generator as seen in Equations (55) and (56) was not carried out, but the author anticipates it would lead to significant changes in the investment planning outcomes. Moreover, by modelling these complex constraints and the interactions between electricity and hydrogen vectors, the framework provided insights into the interactions between these energy vectors and managed the possibility of overestimating or underestimating the actual capacity of flexible technologies required to support the system in the integration of low-carbon technologies and during diverse operational challenges [32]. This was specifically observed in changes in the capacity investments for wind, H_2CCGT plants, blue and green hydrogen plants, and hydrogen storage when the additional constraints were integrated.

7.1 | Computation time

The detailed modelling approach increased the computational complexity of the model, as highlighted by the number of constraints and variables highlighted in Table 1. The large number of constraints and variables greatly impacted the computation (CPU) time as the deterministic MIQP model solved in the range of time, as shown in Table 9. Compared to the model without the detailed scheduling constraints, the model with detailed scheduling constraints required a CPU time of 16 h 30 m to solve for optimality (0.001% Gap). The computation time is reduced by approximately 1 h when removing any of the frequency security constraints. Moreover, the model's performance shows that the detailed scheduling constraints largely impact the computation time. This computational performance highlights great consideration would need to be given to the trade-off between achieving a more accurate estimate of investment results and the amount of time required to solve such a model to optimality.

MIP problems are generally NP-hard, but this model has been enhanced with tight and compact detailed UC constraints and additional constraints removing the symmetries due to the potential presence of multiple identical generators. Experimental testing, as shown in the reported studies, demonstrates

TABLE 9 Model computation time.

Model	CPU time	Relative gap
Model without scheduling constraints	10 s	0.00%
Model with scheduling constraints	16 h 30 m	0.00%
Model without nadir constraints	15 h 19 m	0.00%
Model without frequency security constraints	14 h 17 m	0.00%

the model performs well, reducing the likelihood of overestimating the investment solution.

8 | CONCLUSION

This paper investigates the impact of detailed frequency stability and mixed integer UC constraints, amongst other operational details, on a power system planning problem. A novel integrated planning framework was proposed to identify optimal technology portfolios for a cost-effective electricity system while ensuring frequency stability and reserve requirements. The studies concurrently optimised investments in low-carbon technologies while minimising the system's short-term OC through hourly time resolution representation of the system operation alongside reserve, frequency stability and regulation requirements for a net-zero GB system. The outcome of the studies highlighted the importance of detailed operational constraints for accurately estimating the optimal low-carbon technologies needed in a net-zero system. The results obtained provided optimal and significant trade-offs and cost-effective investment portfolios, from including detailed modelling of UC scheduling and frequency stability constraints versus not including them in a power systems planning problem. The trade-offs were observed in the increased system's costs, based on additional investment in flexible technologies, especially H_2CCGT plants, battery storage, and other hydrogen production and storage technologies required to manage the system should any operational challenges such as the loss of the largest generator occur. The results also emphasised that the system can experience higher annual TC than anticipated due to high demand curtailment by making investment decisions without considering frequency constraints and a detailed UC. The curtailments were observed during periods of low wind generation and when the system required a quick ramping response from flexible power generators. The studies showed that an investment planning framework without frequency security constraints for managing frequency imbalance and detailed modelling of the UC scheduling constraints would lead to resource inadequacy and an underestimation of the technology portfolio required in a net-zero system.

Future work will involve further investigation of the trade-offs and optimal portfolio based on modelling emerging technologies, which can support the flexibility needs of low-carbon power systems in terms of frequency response, systems inertia, and spinning reserve. In addition, future work will include actual grid networks and consider spatial frequency variability and network security constraints. The study will also evolve to carry out a stochastic analysis based on introducing short-term uncertainties in renewable generation or demand. With the solution of this scale of framework being very complex, uncertainty sources can be considered by adding robust margins to different system requirements such as the spinning reserve and frequency response requirements, similarly employed by the authors in Ref. [39]. Another example of an uncertainty source is to add a reserve margin to the generator loss P_t^L estimated by considering the statistical property of a variable generator loss. Using robust margins introduces conservativeness when considering uncertainties, but in complex models, it is inevitable. Future works will also include conducting sensitivity analysis on using a dynamic power in-feed loss compared to a fixed power in-feed loss.

ACKNOWLEDGEMENTS

Olayinka Ayo would like to acknowledge the Petroleum Development Fund (PTDF) for their funding of the research.

CONFLICT OF INTEREST STATEMENT

The authors declare no potential conflict of interests.

DATA AVAILABILITY STATEMENT

The data that support the findings of this study are available on request from the corresponding author. The data are not publicly available due to privacy or ethical restrictions.

ORCID

Olayinka Ayo https://orcid.org/0000-0002-7473-8740

REFERENCES

1. Climate Change Committee oC: The Sixth Carbon Budget: The UK's Path to Net Zero. tech. rep., Report (2020)
2. Strbac, G., et al.: Role and value of flexibility in facilitating cost-effective energy system decarbonisation. Prog. Energy 2(4), 042001 (2020). https://doi.org/10.1088/2516-1083/abb216
3. Strbac, G., et al.: Delivering future-proof energy infrastructure Report for. Natl Infrastruct Comm., 54 (2016)
4. Grid, N.: Future energy scenarios. Report (2020)
5. Strbac, G., et al.: Value of Flexibility in a Decarbonised Grid and System Externalities of Low-Carbon Generation Technologies for the Committee on Climate Change NERA Project Team. Tech. Rep., Imperial College, London (2015)
6. Zhang, X., et al.: Whole-system assessment of the benefits of integrated electricity and heat system. IEEE Trans. Smart Grid 10(1), 1132–1145 (2019). https://doi.org/10.1109/tsg.2018.2871559
7. Pudjianto, D., et al.: Whole-systems assessment of the value of energy storage in low-carbon electricity systems. IEEE Trans. Smart Grid 5(2), 1098–1109 (2014). https://doi.org/10.1109/tsg.2013.2282039
8. Paturet, M., et al.: Stochastic unit commitment in low-inertia grids. arXiv preprint arXiv:1904.03030 (2019)
9. Baik, E., et al.: What is different about different net-zero carbon electricity systems? Energy Clim. Change 2, 100046 (2021). https://doi.org/10.1016/j.egycc.2021.100046
10. Helistö, N., et al.: Impact of operational details and temporal representations on investment planning in energy systems dominated by wind and solar. Appl. Energy 290, 116712 (2021). https://doi.org/10.1016/j.apenergy.2021.116712
11. Schwele, A., Kazempour, J., Pinson, P.: Do unit commitment constraints affect generation expansion planning? A scalable stochastic model. Energy Syst. 11(2), 247–282 (2020). https://doi.org/10.1007/s12667-018-00321-z
12. Morales-España, G., et al.: Power-capacity and ramp-capability reserves for wind integration in power-based UC. IEEE Trans. Sustain. Energy 7(2), 614–624 (2015). https://doi.org/10.1109/tste.2015.2498399

13. Tejada-Arango, D.A., et al.: Power-based generation expansion planning for flexibility requirements. arXiv preprint arXiv:1902.07779 (2019)
14. Tejada-Arango, D.A., et al.: Which unit-commitment formulation is best? A comparison framework. IEEE Trans. Power Syst. 35(4), 2926–2936 (2019). https://doi.org/10.1109/tpwrs.2019.2962024
15. Poncelet, K., Delarue, E., D'haeseleer, W.: Unit commitment constraints in long-term planning models: relevance, pitfalls and the role of assumptions on flexibility. Appl. Energy 258, 113843 (2020). https://doi.org/10.1016/j.apenergy.2019.113843
16. Morales España, G.A., Tejada Arango, D.A.: Modelling the Hidden Flexibility of Clustered Unit Commitment (2019)
17. National Grid: System Needs and Product Strategy. Tech. Rep., National Grid Plc, Warwick (2017)
18. Aurecon: Hornsdale Power Reserve: Year 1 Technical and Market Impact Case Study. tech. rep., Australia (2018)
19. Badesa, L., Teng, F., Strbac, G.: Simultaneous scheduling of multiple frequency services in stochastic unit commitment. IEEE Trans. Power Syst. 34(5), 1–11 (2019). https://doi.org/10.1109/tpwrs.2019.2905037
20. Teng, F., Strbac, G.: Understanding of the flexibility from combined cycle gas turbine plant. In: Badescu, V., Lazaroiu, G.C., Barelli, L. (eds.) Power Engineering: Advances and Challenges, Part A: Thermal, Hydro and Nuclear Power. Taylor and Francis Group (2018).26
21. Wogrin, S., et al.: Assessing the impact of inertia and reactive power constraints in generation expansion planning. Appl. Energy 280, 115925 (2020). https://doi.org/10.1016/j.apenergy.2020.115925
22. Kushwaha, P., et al.: Assessment of energy storage potential for primary frequency response adequacy in future grids. In: 2018 8th IEEE India International Conference on Power Electronics (IICPE), pp. 1–6 (2018)
23. Gonzalez-Longatt, F., et al.: Investigation of inertia response and rate of change of frequency in low rotational inertial scenario of synchronous dominated system. Electronics 10(18), 2288 (2021). https://doi.org/10.3390/electronics10182288
24. Morales-España Jml, G., Ramos, A.: Tight and compact MILP formulation for the thermal unit commitment problem. IEEE Trans. Power Syst. 28(4), 4897–4908 (2013). https://doi.org/10.1109/tpwrs.2013.2251373
25. Gurobi Optimization, L.: Gurobi Optimizer Reference Manual (2021)
26. Sepulveda, N.A., Jenkins, J.D.: Enhanced decision support for a changing electricity landscape: the GenX configurable electricity resource capacity expansion model. In: Preparation for Publication, pp. 1–40 (2017)
27. Moreira, A., Street, A., Arroyo, J.: Energy and reserve scheduling under correlated nodal demand uncertainty: an adjustable robust optimization approach. Int. J. Electr. Power Energy Syst. 72, 91–98 (2015). https://doi.org/10.1016/j.ijepes.2015.02.015
28. Fu, P., et al.: Integration of hydrogen into multi-energy systems optimisation. Energies 13(7), 1606 (2020). https://doi.org/10.3390/en13071606
29. Garifi, K., et al.: Convex relaxation of grid-connected energy storage system models with complementarity constraints in DC OPF. IEEE Trans. Smart Grid 11(5), 4070–4079 (2020). https://doi.org/10.1109/tsg.2020.2987785
30. Gentile, C., España, G.M., Ramos, A.: A tight MIP formulation of the unit commitment problem with start-up and shut-down constraints. EURO J. Comput. Optim. (2016)
31. Teng, F., Trovato, V., Strbac, G.: Stochastic scheduling with inertia-dependent fast frequency response requirements. IEEE Trans. Power Syst. 31(2), 1557–1566 (2016). https://doi.org/10.1109/tpwrs.2015.2434837
32. Helistö, N., et al.: Including operational aspects in the planning of power systems with large amounts of variable generation: a review of modeling approaches. Wiley Interdiscipl Rev. Energy Environ. 8(5), e341 (2019). https://doi.org/10.1002/wene.341
33. Collins, S., Deane, J.P., Gallachóir, B.Ó.: Adding value to EU energy policy analysis using a multi-model approach with an EU-28 electricity dispatch model. Energy 130, 433–447 (2017). https://doi.org/10.1016/j.energy.2017.05.010
34. Teng, F., Trovato, V., Strbac, G.: Stochastic scheduling with inertia-dependent fast frequency response requirements. IEEE Trans. Power Syst. 31(2), 1557–1566 (2015). https://doi.org/10.1109/tpwrs.2015.2434837
35. Lever, A., et al.: Flexibility in Great Britain (2021)
36. Hart, W.E., et al.: Pyomo–optimization Modeling in python, vol. 67. Springer Science & Business Media (2017)
37. Hart, W.E., Watson, J.P., Woodruff, D.L.: Pyomo: modeling and solving mathematical programs in Python. Math. Program. Comput. 3(3), 219–260 (2011). https://doi.org/10.1007/s12532-011-0026-8
38. Strbac, G., et al.: Analysis of Alternative UK Heat Decarbonisation Pathways. Imperial College London, London (2018)
39. Sturt, A., Strbac, G.: Efficient stochastic scheduling for simulation of wind-integrated power systems. IEEE Trans. Power Syst. 27(1), 323–334 (2011). https://doi.org/10.1109/tpwrs.2011.2164558

How to cite this article: Ayo, O., Falugi, P., Strbac, G.: An integrated planning framework for optimal power generation portfolio including frequency and reserve requirements. IET Energy Syst. Integr. 6(4), 545–564 (2024). https://doi.org/10.1049/esi2.12152

APPENDIX A

A | NOMENCLATURE

This section introduces the mathematical symbols most recurrently used in the article.

A.0.1 | Sets

Ω_B	Set of demand blocks indexed by b.
Ω_N	Set of system nodes indexed by n.
Ω_G^T	Set of conventional generation technologies indexed by g_T.
Ω_G	Set $\Omega_N \times \Omega_G^T$ of clusters associated to node n and technology g_T indexed by $g = (n, g_T)$.
N_g	Number of the generator within a cluster g.
Ω_I^g	Set of generation units in the cluster $g \in \Omega_G$ indexed by i
Ω_T^b	Set of time periods in the demand block b indexed by t.
Ω_R^T	Set of candidate renewable technologies.
Ω_R	Set of all renewables indexed by r.
Ω_S	Set of all storage technologies indexed by s.
Ω_S^E	Subset of electricity storage technologies $\left(\Omega_S^E \subseteq \Omega_S\right)$ indexed by es.
Ω_S^H	Subset of H_2 storage technologies $\left(\Omega_S^H \subseteq \Omega_S\right)$ indexed by hs.
Ω_{EL}^T	Set of electrolyser candidate technologies.
Ω_{BL}^T	Set of blue hydrogen candidate technologies.

A.0.2 | Parameters

$d_{t,n}$	Demand (MW) at node n and time t.
$I_{n,\ell}$	Bus-to-line incidence matrix of size $\lvert\Omega_N\rvert \times \lvert\Omega_L\rvert$. $I_{n,\ell} = 1$ if line ℓ is from the sending bus node n $I_{n,\ell} = -1$ if line ℓ is from the receiving bus node n $I_{n,\ell} = 0$ otherwise
$\tilde{h}_s^0$	Initial state-of-charge of the storage device s.
$J_{n,g}$	Bus-to-generation cluster incidence matrix ($\lvert\Omega_N\rvert \times \lvert\Omega_G\rvert$).

$J_{n,g} = 1$ if generator g connects to bus n.
$J_{n,g} = 0$ otherwise
$\overline{h}_{es}$ Maximum charge/discharge rate (MW) of storage es.
ρ_{es} Charging/discharging efficiency of storage es.
N_g Maximum number of generator units within the cluster g.
$\overline{P}_g$ Maximum power output (MW) of a conventional generator unit g.
$\overline{G}_{n,g_T}$ Maximum number of investments in conventional generators of technology g_T at bus node n.
p_g^{msg} Minimum stable generation (MW) of the cluster unit g.
Γ System balance penalty constant (\$/MWh).
Υ Reserve penalty constant (\$/MWh).
κ_o^{ℓ} Annual fixed capital cost (\$/(km yr)) of line ℓ, option o.
κ_r^R Annual capital cost ($/yr) of renewable technology r.
κ_{es}^H Annual capital cost ($/yr) of storage devices es.
κ_g^G Annual capital cost ($/yr) of the generator cluster unit g.
κ_{el}^H Annual capital cost ($/yr) of the electrolyser unit el.
κ_{hs}^H Annual capital cost ($/yr) of hydrogen storage unit hs.
c_g^{su} Start-up cost (\$) of the generator cluster unit g.
c_g^{sd} Shut-down cost (\$) of the generator cluster unit g.
c_g^{nl} No-load cost (\$/h) of the generator cluster unit g.
c_g^G Operation cost ($/MWh) of the generator cluster unit g.
c_s^- Discharging cost ($/MWh) of the storage unit s.
c_s^+ Charging cost ($/MWh) of the storage unit s.
c_{hs}^- H_2 consumption cost ($/MW) of the storage unit hs.
c_{hs}^+ H_2 production cost ($/MW) of the storage unit hs.
c_{el} H_2 production cost ($/MW) by the electrolyser unit el.
c_{bl} H_2 production cost ($/MW) by blue H_2 unit bl.
c_{res} Cost ($/MW) of reserve scheduling.
T_g^{md} Minimum down time (h) of the generator cluster unit g.
T_g^{mu} Minimum up time (h) of the generator cluster unit g.
$\overline{\eta}_{es}$ Energy capacity (MWh) of storage es.
η_{el} Conversion efficiency of the electrolyser el.
η_{hs} Conversion Efficiency of H_2 storage hs.
η_{h2} Conversion efficiency of the H_2CCGT.
RU_g Ramp-up limit (MW/h) of unit g.
RD_g Ramp-down limit (MW/h) of unit g.
$\hat{S}_{es}^-$ Total discharge capacity (MW) of storage es.
SU_g Start-up capability (MW) of the generator cluster unit g.
SD_g Shut-down capability (MW) of the generator cluster unit g.
w_b weight of the demand block b.
t_b^+ First period of the demand block b.
t_b^- Last period of the demand block b.
E^T Annual emission limit (kg/MWh).
$\Delta f_{\max}$ Maximum admissible frequency deviation.
$\Delta f_{\max}^{ss}$ Maximum quasi-steady state frequency deviation.
D Load-damping factor ($Hz).
f_0 Nominal frequency (Hz) of the power grid.
H_g Inertia constant (s) of the generator cluster unit g.
H_L Inertia constant (s) of the generator producing P_t^L.
$P_L^{\max}$ Bound of the largest power in-feed (MW).
$\overline{RoCoF}$ Maximum admissible RoCoF (Hz/s).
T_g Delivery time (s) of PFR.
T_{es} Delivery time (s) of EFR.
P_t^D Total demand (MW) at time t.
Δ_t^{hs} H_2 storage duration (hours).
Δf_{nadir} Frequency at nadir in Hz.

A.0.3 | Decision variables

All decision variables, denoted as x, are as follows:

G_{n,g_T} Candidate (integer) generators of technology g_T at bus n.
$H_{n,es}$ Candidate storage es at bus n.
$R_{n,r}$ Candidate renewable technology r at bus node n.
$G_{n,el}^H$ Candidate electrolyser el at bus n.
$G_{n,bl}^H$ Candidate blue H_2 technologies bl at bus n.
$\overline{S}_{n,hs}$ Candidate H_2 storage hs at bus n.
$p_{t,g}$ Cluster generator power output (MW) at time t.
$\tilde{p}_{t,g,i}$ Power output (MW) above the minimum output of generator unit i in cluster g at time t.
$P_{t,g}$ Total cluster generator power output (MW) at time t.
$Q_{t,n,el}$ Green H_2 production (MW) at time t.
$Q_{t,n,bl}$ Blue H_2 production (MW) at time t.
$p_{t,n,r}^R$ Power output (MW) of renewable r at bus n and time t.
$f_{t,\ell}$ Power flow in line ℓ at time t.
$\theta_{t,n}$ Bus angle at node n and time t.
$h_{t,es}^+$ Power charge of storage es at time t.
$h_{t,es}^-$ Power discharge of storage es at time t.
$\tilde{h}_{t,es}$ State of charge of storage es at time t.
$h_{t,n,hs}^+$ H_2 production by H_2 storage hs at bus n and time t.
$h_{t,n,hs}^-$ H_2 consumed by H_2 storage hs at bus n and time t.
$\tilde{h}_{t,n,hs}$ Energy content of H_2 storage hs at bus n and time t.
$rsp_{t,g}$ Frequency response provided by the cluster generator g (MW) at time t.
$\tilde{rsp}_{t,g,i}$ Frequency response provided by the generator unit i in cluster g at time t.
$res_{t,g}$ Spinning reserve provided by the cluster generator g (MW) at time t.
$\tilde{res}_{t,g,i}$ Spinning reserve provided by generator i in cluster g (MW) at time t.
$u_{t,g}$ Integer variable for the commitment of the number of generator units in cluster g at time t.
$\tilde{u}_{t,g,i}$ Binary variable of unit i in cluster g at time t. It is 1 if unit i is producing above minimum output and 0 otherwise.
$u_{t,g}^+$ Start-up of unit g at time t. It takes 1 if unit starts up at time t and 0 otherwise.
$u_{t,g}^-$ Shut-down of unit g at the operating point t. it takes 1 if unit shuts down at time t and 0 otherwise.
$\hat{\alpha}_{es,t}^{rsp}$ Proportion of storage charging that can be interrupted to provide the frequency response.

$\hat{\alpha}_{es,t}^{res}$ Proportion of storage charging that can be interrupted to provide operating reserves.
R_t^{slack} Reserve curtailment (MW) at the operating point t.
P_t^L Largest power in-feed (MW) at time t.
H_t System inertia (MWs) after the loss of P_t^L.
R_t^G Total PFR (MW) from all generators.
R_t^{ES} Total EFR (MW) from all storage units.